1992

Using nonlinear sensitivities to estimate eigenvalues and eigenvectors for large design changes

Judith Marie Callicott Vance
Iowa State University

Order Number 9223972

Using nonlinear sensitivities to estimate eigenvalues and eigenvectors for large design changes

Vance, Judith Marie Callicott, Ph.D.

Iowa State University, 1992

U·M·I
300 N. Zeeb Rd.
Ann Arbor, MI 48106

Using nonlinear sensitivities to estimate eigenvalues and eigenvectors for large design changes

by

Judith Marie Callicott Vance

A Dissertation Submitted to the
Graduate Faculty in Partial Fulfillment of the
Requirements for the Degree of
DOCTOR OF PHILOSOPHY

Major: Mechanical Engineering

Approved:

Signature was redacted for privacy.

In Charge of Major Work

Signature was redacted for privacy.

For the Major Department

Signature was redacted for privacy.

For the Graduate College

Iowa State University
Ames, Iowa
1992

TABLE OF CONTENTS

ACKNOWLEDGEMENTS viii

CHAPTER 1. INTRODUCTION 1

CHAPTER 2. LITERATURE REVIEW 3

Methods for Estimating Modes Shapes and Frequencies 4

Power Series for Eigenvalues and Eigenvectors Used in Interactive Design . 5

Estimating Eigenvalues and Eigenvectors Using Padé Approximants 8

Estimating Eigenvalues and Eigenvectors Using Curve Fit Techniques . . . 8

Efficient Methods of Calculating Eigenvalue and Eigenvector Derivatives . 8

CHAPTER 3. SENSITIVITY ANALYSIS PROCEDURE FOR DYNAMIC STRUCTURAL DESIGN 12

Eigenvalue and Eigenvector Derivatives 12

Power Series Approximation of Eigenvalues and Eigenvectors 15

Padé Approximants 16

Curve Fit Techniques 18

CHAPTER 4. A SIMPLE EXAMPLE: A TWO DEGREE-OF-FREEDOM MODEL 20

Power Series Approximation of Eigenvalues and Eigenvectors 20

Padé Approximants of Eigenvalues 28
Curve Fit Approximations of Eigenvalues and Eigenvectors 31
Using the Inner Product to Identify Eigenvalue Match 34
Using Cut Off Percents to Determine When to Re-solve 43
CHAPTER 5. FINITE ELEMENT MODEL 49
Power Series Approximations 51
Padé Approximants 57
Using Inner Product Matching for High Frequencies 61
Comparison of Power Series Methods to Padé Approximant Methods . . . 65
CHAPTER 6. CONCLUSIONS AND FUTURE WORK 69
BIBLIOGRAPHY 71

LIST OF TABLES

Table 4.1: Inner product of $(U_m^*)^T M U_p$ for $m1 = 3.0$ 38

Table 4.2: Inner product of $(U_m^*)^T M U_p$ for $m1 = 2.0$ 38

Table 4.3: Mode 1: Number of re-solves needed for solution 44

Table 4.4: Mode 2: Number of re-solves needed for solution 45

Table 4.5: Mode 1: $m1$ values resulting from 2% cut off re-solve criterion 45

Table 4.6: Mode 2: $m1$ values resulting from 2% cut off re-solve criterion 45

Table 5.1: Properties for the square plate model 50

Table 5.2: Mode 1 inner product of $(U_1^*)^T M U_p$ for $t_l = 1.20\ mm$ 52

Table 5.3: Mode 2 inner product of $(U_2^*)^T M U_p$ for $t_l = 0.776\ mm$ 53

Table 5.4: Mode 2 inner product of $(U_2^*)^T M U_p$ for $t_l = 1.20\ mm$ 55

Table 5.5: Mode 1 inner product of $(U_1^*)^T M U_p$ for $t_l = 1.20\ mm$ using Padé estimates 60

Table 5.6: Mode 2 inner product of $(U_2^*)^T M U_p$ for $t_l = 1.20\ mm$ using Padé estimates 61

Table 5.7: Mode 9 inner product of $(U_9^*)^T M U_p$ for $t_l = 0.648\ mm$ 63

Table 5.8: Mode 9 inner product of $(U_9^*)^T M U_p$ for $t_l = 0.922\ mm$ 63

Table 5.9: Mode 9 inner product of $(U_9^*)^T M U_p$ for $t_l = 1.20\ mm$ 64

Table 5.10: Computation time required for Padé method and power series methods for mode 2 68

LIST OF FIGURES

Figure 4.1: Two degree-of-freedom system 20
Figure 4.2: Mode 1 power series approximation (up to 4 terms) 22
Figure 4.3: Mode 2 power series approximation (up to 4 terms) 23
Figure 4.4: Mode 2 power series approximation (up to 100 terms) 24
Figure 4.5: Mode 1 power series approximation (up to 100 terms) 25
Figure 4.6: Mode 1 power series approximation of eigenvector $u11$ 26
Figure 4.7: Mode 1 power series approximation of eigenvector $u12$ 27
Figure 4.8: Mode 2 power series approximation of eigenvector $u21$ 29
Figure 4.9: Mode 2 power series approximation of eigenvector $u22$ 30
Figure 4.10: Mode 1 Padé approximation 32
Figure 4.11: Mode 2 Padé approximation 33
Figure 4.12: Mode 1 cubic and fifth-order approximations 35
Figure 4.13: Mode 2 cubic and fifth-order approximations 36
Figure 4.14: Mode 1 eigenvalue approximation using inner product matching: re-solve at $m1 = 2.0$ 39
Figure 4.15: Mode 2 eigenvalue approximation using inner product matching: re-solve at $m1 = 2.0$ 40

Figure 4.16: Mode 1 eigenvector approximation using inner product matching: re-solve at $m1 = 2.0$ 41

Figure 4.17: Mode 2 eigenvector approximation using inner product matching: re-solve at $m1 = 2.0$ 42

Figure 4.18: Mode 1 curve fit between re-solve points: using inner product matching 48

Figure 5.1: The plate model 49

Figure 5.2: Mode 1 power series approximation: no re-solves 54

Figure 5.3: Mode 2 power series approximation: re-solve at $t = 0.776\ mm$ 56

Figure 5.4: Mode 2 nodal displacement along a plate cross-section for $t = 0.65\ mm$ 58

Figure 5.5: Mode 2 nodal displacement along a plate cross-section for $t = 1.0\ mm$ 59

Figure 5.6: Mode 2 Padé approximants: no re-solves 62

Figure 5.7: Mode 9 Padé and power series approximations 66

ACKNOWLEDGEMENTS

I wish to express my gratitude to Dr. James Bernard for his guidance and friendship throughout my graduate studies. I want to particularly thank him for his constant encouragement and support. It was a privilege to work with him.

I also wish to thank the members of my graduate committee, Dr. Bion Pierson, Dr. Tom Rudolphi, Dr. Martin Vanderploeg, and Dr. James Wilson. Their suggestions on this work were very appreciated.

Finally, I wish to thank my husband, Bruce, and our children, Shelly and Kyle, for their understanding, patience, and loving support.

CHAPTER 1. INTRODUCTION

Finite element analysis is frequently used to determine the dynamic characteristics of physical systems. Usually a current design is modeled using finite element analysis and the calculated results are compared to design goals. If the comparison indicates that the design is unsuitable, the model is changed and the analysis is performed again. The re-design/re-analysis cycle is repeated until a viable design is achieved.

The iterative task of arriving at a suitable design can be cast into an optimization problem. Based on so-called design parameters, an objective function can be created which takes into account the desired response of the system, and constraints can be developed to impose limits on the design parameters. Then an optimization algorithm can be used to arrive at the optimal design. For large systems, the finite element analysis that is part of the optimization can be computationally intensive, causing the re-design/re-analysis cycle to be very time consuming.

Because of the lengthy time involved in numerical optimization of large systems, input from the designer during such an optimization process is very limited. This can be a serious shortcoming because the constraints governing the final design are usually not clear-cut. Keeping the designer in the design loop would allow judgements to be made regarding the relative importance of conflicting constraints.

This dissertation presents a method to replace repeated finite element runs with an easy-to-compute approximation for eigenvalues and eigenvectors which can be performed interactively and thereby allow the designer to stay in control of the process. In addition, the case is made for combining approximations with interactive computer graphics to provide design engineers with a powerful design tool. The ability to see the mode shape vibrating on the screen, then change a design parameter and see an estimation of the new mode shape displayed on the screen helps the design engineer gain a deeper understanding of the system. The development of an efficient, accurate approximation for the eigenvectors and eigenvalues is essential to obtaining such an interactive design environment.

Chapter 2 presents a review of literature dealing with approximating mode shapes and frequencies and derivative calculations of eigenvalues and eigenvectors. Chapter 3 presents the details of several approximating methods. Chapter 4 compares the results of several methods in the context of a simple problem. Chapter 5 presents the results of several methods applied to a much more complicated problem. Chapter 6 presents conclusions and a discussion of future work.

CHAPTER 2. LITERATURE REVIEW

Structural design often involves optimization problems in which the objective function includes the solution to an eigenvalue problem of the form

$$[K(e) - \lambda(e)M(e)]U(e) = 0.0 \tag{2.1}$$

where e is a design parameter or a vector of design parameters. For a system with n degrees-of-freedom, $M(e)$ is the nxn symmetric mass matrix, $K(e)$ is the nxn symmetric stiffness matrix, $\lambda(e)$ is the eigenvalue, and $U(e)$ is the n-length eigenvector. Both the mass and stiffness matrices have real elements dependent on the independent variable(s) e. In practice, equation (2.1) is often obtained by modeling the system using a finite element preprocessor, then the equation is solved to produce eigenvalues and eigenvectors of the system using any of a variety of eigenvalue solvers.

For systems with a large number of degrees of freedom, the solution to equation (2.1) is computationally intensive [1]. It is therefore in the interest of the designer to obtain the optimal design with as few re-solutions as possible. This has led to the need for methods to estimate eigenvalues and eigenvectors as a function of design change.

Methods for Estimating Modes Shapes and Frequencies

Power series approximations of eigenvalues and eigenvectors are based on a Taylor series expansion about an original design point. The power series for the eigenvalue, λ, and the eigenvector U with respect to a single design change , e, may be written

$$\lambda(e) = \sum_{n=0}^{\infty} \lambda^{(i)} (\Delta e)^i \tag{2.2}$$

$$U(e) = \sum_{n=0}^{\infty} U^{(i)} (\Delta e)^i \tag{2.3}$$

where the superscript (i) indicates the series coefficient and

$$\lambda^{(i)} = \frac{\left(\frac{d^i \lambda}{de^i}\right)}{i!} \tag{2.4}$$

The technique of using power series approximations of eigenvalues was first presented by Wittrick [2] and applied to buckling of a thin plate. He based his work on Jacobi's [3] derivation of the eigenvalue derivatives of symmetric eigenproblems of the standard form

$$Ax = B \tag{2.5}$$

with A symmetric and $B = I$. Lancaster [4] presented a comprehensive treatment of both eigenvalue and eigenvector derivatives of nonsymmetric standard eigenproblem systems including the derivation of the second eigenvalue derivative and a discussion of both distinct and repeated eigenvalue systems. Fox and Kapoor [5] presented two methods for calculating the first derivative of the eigenvector for the generalized eigenproblem

$$Kx = \lambda Mx \tag{2.6}$$

with real, symmetric M and K. The first method, a result of direct differentiation, requires inverting an nxn matrix but only involves the eigenvalue and eigenvector of interest. In contrast, the second method assumes the eigenvector derivative is a linear combination of all of the eigenvectors of the system. These methods were later expanded by Rogers [6] to include nonsymmetric systems. The second derivative of the eigenvalue of nonsymmetric systems was presented by Plaut and Huseyin [7]. Rudisill and Bhatia [8], derived expressions for the second derivative of the eigenvalues of complex systems.

More recently, derivations of n^{th} order eigenvalue and eigenvector derivatives of symmetric systems, nonsymmetric systems and systems with repeated eigenvalues have been developed. Summaries of developments in eigenvalue and eigenvector derivative calculations have been published by Adelman and Haftka [1], and Murthy and Haftka [9].

Power Series for Eigenvalues and Eigenvectors Used in Interactive Design

Storaasli and Sobieszczanski [10] demonstrated how the linear Taylor series could be used as an approximation to the static equation

$$Kx = F \tag{2.7}$$

to approximate displacements and stresses in an aircraft fuselage. In this equation, K is the nxn stiffness matrix for a system with n degrees-of-freedom, x is a vector of nodal displacements, and F is the force vector. The linear Taylor series is formed for the displacement x with respect to design variable e

$$x(e + \Delta e) = x(e) + (\delta x/\delta e)(\Delta e) \tag{2.8}$$

They used this approximation to estimate displacement and stress changes in the skin of the fuselage which resulted from changes in skin thickness, cross-sectional areas of stringers and from simultaneous changes in area, torsional and bending inertias for the frames. Kirsch [11] presents a survey of static structural reanalysis methods based on series expansion.

The shortcoming of the linear approximations is that the relationship between eigenvalues and design parameters is not likely to be linear and therefore the linear approximation may be valid only for small changes in the design parameter. To overcome this problem, higher-order sensitivity analysis has been investigated. Sensitivity analysis involves determining the change in the eigenvalues and eigenvectors with respect to a given design change. Haug [12], Haftka [13], Vanderplaats and Yoshida [14], and Sobieszczanski-Sobieski [15] examined the effect of second-order sensitivity analysis on the statics problem of equation (2.7).

Rizai and Bernard [16] investigated using higher-order terms in the Taylor series to estimate the eigenvalues of a beam with fixed ends. They used a 9-term Taylor series

$$\lambda(e + \Delta e) = \lambda(e) + \sum_{i=1}^{8} \lambda^{(i)} (\Delta e)^i \tag{2.9}$$

where e was the design variable and

$$\lambda^{(i)} = \frac{\left(\frac{d^i \lambda}{de^i}\right)}{i!} \tag{2.10}$$

Although they often achieved good approximations over a large design range, some of the approximations were limited by the radius of convergence of the Taylor series. They proposed a re-solution and re-approximation procedure to overcome the convergence difficulties.

Optimization with respect to one design variable can be formulated into a nonlinear Taylor series, but in practice it is rare to find a design that is only dependent on one design variable. When many design variables are involved, using a nonlinear Taylor series can become unmanageable due to the cross derivatives involved in the series expansion. However, a linear Taylor series is only applicable to small design changes.

Rizai and Bernard [16] proposed using a combination of linear and nonlinear series approximations in an optimization process when the design decisions involve multiple design parameters. Their method involves first using a linear approximation of the eigenvalues and eigenvectors as a function of the design variables, e^i, in the context of a penalty function optimization procedure. The optimization results in an estimate of the best combination of design parameters, $\overline{e}^i$ if the eigenvalues were linear in the design parameters. Then a new design variable, ϵ, is introduced such that

$$e^i = \epsilon \overline{e}^i \tag{2.11}$$

The optimization proceeds based on a nonlinear Taylor series in ϵ. This relationship, equation (2.11) establishes the assumption that the best set of design parameters that result from the nonlinear eigenvalue approximation is a scalar multiple of the $\overline{e}^i$ found from the linear eigenvalue optimization. The radius of convergence of the Taylor series still caused difficulties in the nonlinear series approximation. Gopi Somayajula [17] applied this optimization scheme to several problems.

This thesis focuses on the second part of that procedure, which involves nonlinear approximations of the eigenvalues and eigenvectors with respect to one design variable.

Estimating Eigenvalues and Eigenvectors Using Padé Approximants

To avoid the convergence problems of the Taylor series approximations, Whitesell [26] proposed using Padé Approximants to estimate the eigenvalues and eigenvectors of a modified system. He showed that the use of Padé Approximants can extend the validity of the approximation well beyond the convergence difficulties experienced when using the Taylor series. Kwon [27] applied Padé approximants to the statics problem of $Kx = F$ and achieved promising results. This thesis will extend that work and apply Padé approximants to dynamics problems.

Estimating Eigenvalues and Eigenvectors Using Curve Fit Techniques

Vance and Bernard [28] took another approach to estimating eigenvalues and eigenvectors with respect to a design change. They proposed using a curve fit between widely spaced solutions to span the entire range of the possible design changes. Although the method required a re-solution of the system equations at the far end of the design range, it was shown to provide a good approximation for a fairly complex example across the design range without additional re-solves. Reference [28] considered both a cubic power series and a fifth-order curve fit approximation for eigenvalues and eigenvectors over a large design range.

Efficient Methods of Calculating Eigenvalue and Eigenvector Derivatives

The power series, Padé approximants and curve fit techniques all depend on calculation of eigenvalue and eigenvector derivatives. Adelman and Haftka [1] state that calculation of the derivatives of the system equations represent the predominant con-

tributor to the excessively long and expensive computer runs required for optimization of large structural systems based on estimates of eigenvalues and eigenvectors. They believe the success of using higher-order power series approximations in an traditional optimization algorithm lies in the efficiency of calculating eigenvalue and eigenvector derivatives. Calculation of eigenvalue first derivatives is fairly straightforward. But calculation of eigenvector derivatives and higher order eigenvalue derivatives is more complicated and computationally costly.

Efficient methods of calculating eigenvalue and eigenvector derivatives were presented by Garg [18] and Rudisill [19]. Garg derived a method for finding the first derivatives of the eigenvectors and eigenvalues of complex systems which requires the solution of $2(n+1)$ equations for a system with n degrees of freedom. Rudisill derived another method for finding the second derivative of the eigenvalues and eigenvectors of non-self-adjoint systems which was similar to Fox and Kapoor's [5] first method. Rudisill's method only requires one right-hand and one left-hand eigenvector of the system instead of a full set of eigenvectors.

Nelson [20] presented a method, based on Fox and Kapoor's [5] first formulation, that simplified calculation of eigenvector derivatives. Nelson's method involves converting the n^{th} order $(n-1)$ rank system of equations to an n^{th} order n rank system by zeroing a row and a column of the original set of equations. His method is applicable to both symmetric and nonsymmetric matrices. In contrast to Nelson's method, Cardani and Mantegazza [21] proposed adding an equation to the derivative equations to make a set of $n+1$ linear equations.

Haug and Arora [22] used the theory of adjoint structures to develop an alternate method of calculating eigenvalue and eigenvector derivatives. Ojalvo [23] expanded

on Nelson's work and included a discussion of eigenvector derivatives of repeated eigenvalues. Whitesell [24] proposed using a generalized inverse of $(K - \lambda M)$ to solve the eigenvector equations. In particular, Whitesell's method allows the calculation of the eigenvector derivatives in $O(n^2)$ operations.

All of these methods require derivatives of the mass and stiffness matrices with respect to the design variable. If the matrices are analytically differentiable these derivatives can be explicitly found. But for many design changes these matrices cannot be formulated analytically and finite difference techniques are needed to obtain the derivatives. However, higher-order derivatives are difficult to obtain using that method. Bernard, Kwon, and Wilson [25] proposed replacing the terms in the mass and stiffness matrices with a cubic curve fit between two design points. This typically has led to a good fit for M and K across the design range. Although this method leads to the assumption that all derivatives of the M and K matrices higher than the third derivative are zero, it does not limit the order of eigenvalue and eigenvector derivatives that can be calculated.

The goal of this thesis is to arrive at an accurate, efficient method of estimating eigenvalues and eigenvectors across a given design range so that interactive design of large systems will become feasible. With the emergence of very fast computer workstations, the hardware is available for animating complicated mode shapes. Fast and accurate numerical methods to estimate eigenvalues and eigenvectors will enable the designer to animate original mode shapes, change a design parameter, and view the new estimated mode shape animated on the screen. Interactive design, based on estimation of eigenvalues and eigenvectors also could be combined with optimization methods, as suggested by Starkey and Bernard [29], and extended by Rizai

and Bernard [16], and Somayajula and Bernard [17], which would take advantage of optimization algorithms, yet keep the designer active in the design process.

This thesis compares power series approximations, Padé approximant methods, and curve fit techniques for systems with a single design parameter of interest. For systems with multiple design parameters, the intent is to develop a method that would facilitate the single parameter optimization step of Rizai and Bernard's method. Comparisons are made for each method in the context of a simple two-degree-of-freedom problem and a much larger finite-element-based problem.

CHAPTER 3. SENSITIVITY ANALYSIS PROCEDURE FOR DYNAMIC STRUCTURAL DESIGN

The purpose for sensitivity analysis in a dynamic structural design context is to approximate the eigenvalues and eigenvectors of the system

$$K(e)U(e) = \lambda(e)M(e)U(e) \tag{3.1}$$

where e is a design parameter. Sensitivity methods are typically applied to large systems where the solution to equation (3.1) is numerically time consuming. The intent is to arrive at a satisfactory approximation to the eigenvalues and eigenvectors in a shorter time than it would take to re-solve the system equations.

This chapter discusses Taylor series expansions, Padé approximants, and curve fit techniques for structural redesign.

Eigenvalue and Eigenvector Derivatives

All of the methods discussed in this thesis require derivatives of eigenvalues and eigenvectors. Whitesell's method [24], which provides the required derivatives in $O(n^2)$ calculations, will be used here.

Whitesell expressed the power series coefficients of the m^{th} eigenvalue as

$$\lambda_m^{(i)} = U_m^T y^{(i)} \tag{3.2}$$

with

$$y^{(i)} = \sum_{j=0}^{i-1} K^{(i-j)} U_m^{(j)} - \sum_{j=0}^{i-1} \left(\sum_{\substack{k=0 \\ k \neq i}}^{i-1} M^{(i-j-k)} \lambda_m^{(k)} \right) U_m^{(j)} \tag{3.3}$$

The derivatives of the eigenvalues with respect to a design change, e, can easily be calculated from the power series coefficients

$$\frac{d^i \lambda_m}{de^i} = i! \lambda_m^{(i)} \tag{3.4}$$

Whitesell proposed using the generalized inverse of $(K - \lambda M)$ to simplify the calculation of the eigenvector power series coefficients, leading to

$$U_m^{(i)} = -(K - \lambda_m M)^I y^{(i)} + C_i U_m \tag{3.5}$$

where $(K - \lambda_m M)^I$ is the generalized inverse of the singular $(K - \lambda_m M)$ matrix. The generalized inverse satisfies the following [24]:

$$(K - \lambda_m M)(K - \lambda_m M)^I (K - \lambda_m M) = (K - \lambda_m M) \tag{3.6}$$

$$(K - \lambda_m M)^I (K - \lambda_m M)(K - \lambda_m M)^I = (K - \lambda_m M)^I \tag{3.7}$$

$$U_m^T M (K - \lambda_m M)^I = 0 \tag{3.8}$$

$$(K - \lambda_m M) M U_m = 0 \tag{3.9}$$

The generalized inverse can be calculated by

$$(K - \lambda_m M)^I = \left(I - \frac{U_m U_m^T M}{U_m^T M U_m} \right) (K - \tilde{\lambda_m} M)^{-1} \left(I - \frac{(I - M U_m U_m^T)}{U_m^T M U_m} \right) \tag{3.10}$$

where I is the unit matrix and $\tilde{\lambda_m} = \lambda_m + \epsilon$. C_i in equation (3.5) is an eigenvector scaling parameter. If the eigenvectors are scaled such that $U_m^T M U_m = 1$ then

$$C_i = -\frac{1}{2} \left[\left(\sum_{k=1}^{i} U_m^{(i-k)^T} M^{(k)} \right) U_m + \sum_{j=1}^{i-1} \left(\sum_{k=0}^{i-j} U_m^{(i-j-k)^T} M^{(k)} \right) U_m^{(j)} \right] \tag{3.11}$$

Derivatives of the mass and stiffness matrices are present in both equation (3.3) and (3.11). Typically the M and K matrices are not easily differentiable and the derivatives must be approximated. Following the procedure laid out by Bernard, Kwon, and Wilson [25], each element in the K and M matrices can be replaced by a cubic function of the design change, e. Let each element, k_{ij}, of the K matrix be replaced by $\overline{k_{ij}}$ such that

$$\overline{k_{ij}} = \sum_{k=0}^{3} a_{ijk}(e - e_o)^k \tag{3.12}$$

with e_o taken at the initial design. Reference [25] recommends defining the coefficients such that at e_o ; $\overline{k_{ij}} = k_{ij}$, $\overline{k_{ij}}' = k'_{ij}$, and $\overline{k_{ij}}'' = k''_{ij}$. In addition, at the other end of the range, at e_{end}, $\overline{k_{ij}}(e_{end}) = k_{ij}(e_{end})$, where the prime notation indicates differentiation with respect to the design variable e. This results in

$$a_{ij0} = k_{ij}(e_o) \tag{3.13}$$

$$a_{ij1} = k'_{ij}(e_o) \tag{3.14}$$

$$a_{ij2} = \frac{k''_{ij}}{2}(e_o) \tag{3.15}$$

$$a_{ij3} = \frac{1}{L^3}(k_{ij}(e_{end}) - a_{ij1} - a_{ij2}L - a_{ij3}L^2) \tag{3.16}$$

where $L = e_{end} - e_o$. The derivatives of K can be found by differentiating equation (3.12). A cubic fit for the mass matrix can be formulated in a similar manner.

The procedure presented by Whitesell for calculating the coefficients for the m^{th} eigenvector of a problem scaled such that $U_m^T M U_m = 1.0$ is

1. Form the LU decomposition of $(K - \tilde{\lambda_m} M)$.

2. Solve for w^i in $L_L w^i = (I - M U_m U_m^T) y^{(i)}$.

3. Solve for p^i in $L_U p^i = w^i$.

4. Calculate $U_m^{(i)} = -(I - U_m U_m^T M)p^i + C_i U_m$.

where $\tilde{\lambda_m} = \lambda_m + \epsilon$. L_L and L_U are the lower and upper triangular matrices obtained in step 1. The two matrices $(I - MU_m U_m^T)$ and $(I - U_m U_m^T M)$ operate on the nearly singular matrix $(K - \tilde{\lambda_m} M)$ to form the generalized inverse $(K - \lambda_m M)^I$.

The LU decomposition is the most expensive operation of the algorithm. However, if the inverse iteration with shift technique is used to solve equation (3.1) for the eigenvalues and eigenvectors, then the LU decomposition of $(K - \tilde{\lambda_m} M)$ is already available and the $\lambda_m^{(i)}$ and $U_m^{(i)}$ can be calculated efficiently.

Whitesell's equations lead to expressions for the power series coefficients. The eigenvector derivatives are scalar multiples of the coefficients and can be calculated using

$$\frac{d^i U_m}{de^i} = i! U_m^{(i)} \tag{3.17}$$

Power Series Approximation of Eigenvalues and Eigenvectors

A Taylor series approximation can be used to estimate eigenvalues and eigenvectors with respect to a design change, e. The series has the form of

$$\lambda_m(e) = \sum_{n=0}^{k} \lambda_m^{(i)} (\Delta e)^i \tag{3.18}$$

$$U_m(e) = \sum_{n=0}^{k} U_m^{(i)} (\Delta e)^i \tag{3.19}$$

where e_o is the initial design parameter and $e = e_o + \Delta e$. In theory, the number of terms chosen for the series, k, could approach infinity. However, in practice, calculation of the coefficients is not a trivial matter.

It is common practice to use a linear approximation of the eigenvalues and eigenvectors [29] where

$$\lambda_m(e) = \lambda_m(e_o) + \lambda_m^{(1)}(e_o)(e - e_o) \tag{3.20}$$

$$U_m(e) = U_m(e_o) + U_m^{(1)}(e_o)(e - e_o) \tag{3.21}$$

Commercial software such as MSC/Nastran [30] provides the ability to calculate these linear coefficients for a wide variety of design changes. Although these linear coefficients do give the designer a better feeling for the nature of the changes that occur in the eigenvalues and eigenvectors in the neighborhood of the original design, the usefulness of the approximations has a limited range. Specifically, the eigenvalues and eigenvectors are rarely linear with respect to a design variable. Therefore several small step re-solves must be performed to get a good approximation across a wide range of design values.

Higher-order power series have also been investigated [16]. While giving better approximations to the eigenvalues and eigenvectors, convergence difficulties may arise due to the fixed radius of convergence inherent in Taylor series expansions.

Padé Approximants

In an attempt to overcome the convergence problems of power series expansions, Whitesell [26] proposed using Padé approximants to estimate eigenvalues and eigenvectors. Padé approximants are rational functions that exhibit superior convergence properties over the Taylor series [31]. The Padé approximant for the formal power series F,

$$F(x) = \sum_{n=0}^{\infty} a_n x^n \tag{3.22}$$

is $R_{l,m}$ where

$$R_{l,m} = \frac{P}{Q} \approx F(x) \tag{3.23}$$

P is an l^{th} order polynomial and Q is an m^{th} order polynomial. A special case exists when $m = 0$. In that case, the Padé approximant is the Taylor polynomial of degree l.

Whitesell [26] introduced an innovative method for solving Padé value problems. The value of the Padé approximant of F is

$$R_{l,m} = \sum_{i=0}^{m} \frac{1}{\eta_i} \tag{3.24}$$

where the η_i follow from the solution to the equation

$$H\eta = e \tag{3.25}$$

where $e^T = [\ 1,\ 1,\ \ldots,\ 1]$. The $(m+1)$x$(m+1)$ matrix H is a matrix of partial sums of the Taylor series.

$$H = \begin{bmatrix} h_l & h_{l-1} & \cdots & h_{l-m} \\ h_{l+1} & h_l & \cdots & h_{l-m+1} \\ \vdots & \vdots & & \vdots \\ h_{l+m} & h_{l+m-1} & \cdots & h_l \end{bmatrix} \tag{3.26}$$

with

$$h_i = \sum_{n=0}^{i} a_n x^n \tag{3.27}$$

When the eigenvalues and eigenvectors of equation (3.1) are expressed using a power series of the form of equation (3.22), the Padé approximant of any order (l, m) can be calculated using equation (3.25), provided the required series coefficients, a_n, are available. The largest order Taylor series required in the H matrix is the $(l+m)^{th}$

order, therefore $l + m + 1$ series coefficients are needed to form $R_{l,m}$. For the $R_{l,m}$ Padé approximant, the original eigenvalue or eigenvector and $l + m$ derivatives are needed to calculate the a_n.

Curve Fit Techniques

Whereas Taylor series approximations require derivatives of the initial design only, curve fit techniques use solution information and derivatives at both the initial design point and at the design configuration at the far end of the design range. To estimate eigenvalues and eigenvectors Vance and Bernard [28] proposed using a fifth-order curve based on the eigenvalue or eigenvector and the first and second eigenvalue and eigenvector derivative at each end of the design range. The eigenvalue would be approximated with

$$\lambda(e) = \sum_{i=0}^{n} a_i (e^*)^i \tag{3.28}$$

for an n^{th} order curve fit. The variable e^* is the normalized design change that varies from 0 to 1 across the interval:

$$e^* = \frac{(e - e_o)}{(e_{end} - e_o)} \tag{3.29}$$

For a fifth-order fit, six pieces of information about the correct solution are needed to calculate the a_i coefficients. The a_i coefficients can be chosen such that the curve fit matches the correct solution at both endpoints of the design range and also has first and second derivatives that match the correct solution at both design endpoints. Therefore

$$a_0 = \lambda(0) \tag{3.30}$$

$$a_1 = \lambda'(0) \tag{3.31}$$

$$a_2 = \lambda''(0)/2.0 \tag{3.32}$$

$$\sum_{i=0}^{5} a_i = \lambda(1) \tag{3.33}$$

$$\sum_{i=1}^{5} i a_i = \lambda'(1) \tag{3.34}$$

$$\sum_{i=2}^{5} i(i-1) a_i = \lambda''(1) \tag{3.35}$$

$$\tag{3.36}$$

The prime denotes the derivative with respect to the variable e. Any order of curve fit can be used provided enough derivatives are available at the initial design point and at the end of the design range.

One advantage of using a curve fit is that the approximation closely matches the correct solution at both ends of the design range. A Taylor series approximation, on the other hand, closely matches the correct solution near the initial design value but it may not converge for large design changes, causing large errors in the approximation.

The next chapter illustrates, in the context of a simple problem, several methods for approximating eigenvalues and eigenvectors. The intent is to arrive at a method that will facilitate the approximation of eigenvalues and eigenvectors of large systems over a range that includes large changes of the design parameters. Such a method would make interactive design feasible.

CHAPTER 4. A SIMPLE EXAMPLE: A TWO DEGREE-OF-FREEDOM MODEL

Figure 4.1 presents a simple system consisting of two masses connected by linear springs. The design change to be considered here is the simultaneous increase of mass 1 and decrease of mass 2 by Δm. The initial design has $m1 = 1.0$, $m2 = 3.0$, and $k1 = k2 = k3 = 1.0$. The range of the design space extends to $m1 = 3.0$ and $m2 = 1.0$.

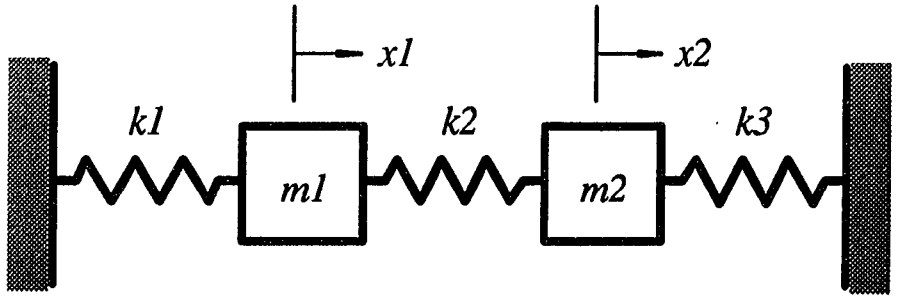

Figure 4.1: Two degree-of-freedom system

Power Series Approximation of Eigenvalues and Eigenvectors

First consider an n^{th} order Taylor series. Figure 4.2 presents results based on using low-order power series to approximate the lowest frequency of the system,

which will be referred to as mode 1. As additional terms are added to the series, the approximation begins to approach the correct solution. The 4-term power series approximates the frequencies in the range quite well.

For mode 2, the calculated results are not as encouraging. Figure 4.3 shows that the low-order series approximates the correct solution only for small design changes.

Since convergence may be limited within the design range by the radius of convergence of the series, the addition of higher-order terms may or may not improve the approximation. For this model, divergence of mode 2 is expected at $\Delta m = 1.0$ corresponding to the radius of convergence surrounding $m1 = 1.0$. However, the point of divergence is not always obvious because the system may also diverge due to the presence of poles in the complex plane.

Figure 4.4 presents the power series expansion of mode 2 using 5 terms, 10 terms, and 100 terms. Addition of more terms to the series results in extending the valid range of the approximation up to the point where the series diverges. Divergence is observed at $m1 = 2.0$ which corresponds to $\Delta m = 1.0$. Figure 4.5 shows similar approximations for the first mode. The 100-term series diverges at $m1 \approx 2.6$. In this case, the point of divergence can not be identified easily before it is observed. This uncertainty about the radius of convergence is a challenge faced by users of high-order Taylor series expansions.

Eigenvector approximations, which are closely related to eigenvalue estimations, exhibit the same difficulties with respect to convergence. Figure 4.6 shows the results of the addition of various terms to the power series for the first eigenvector entry of the first mode ($u11$). Figure 4.7 shows the results of the addition of various terms to the power series for the second eigenvector entry of the first mode ($u12$). Here the

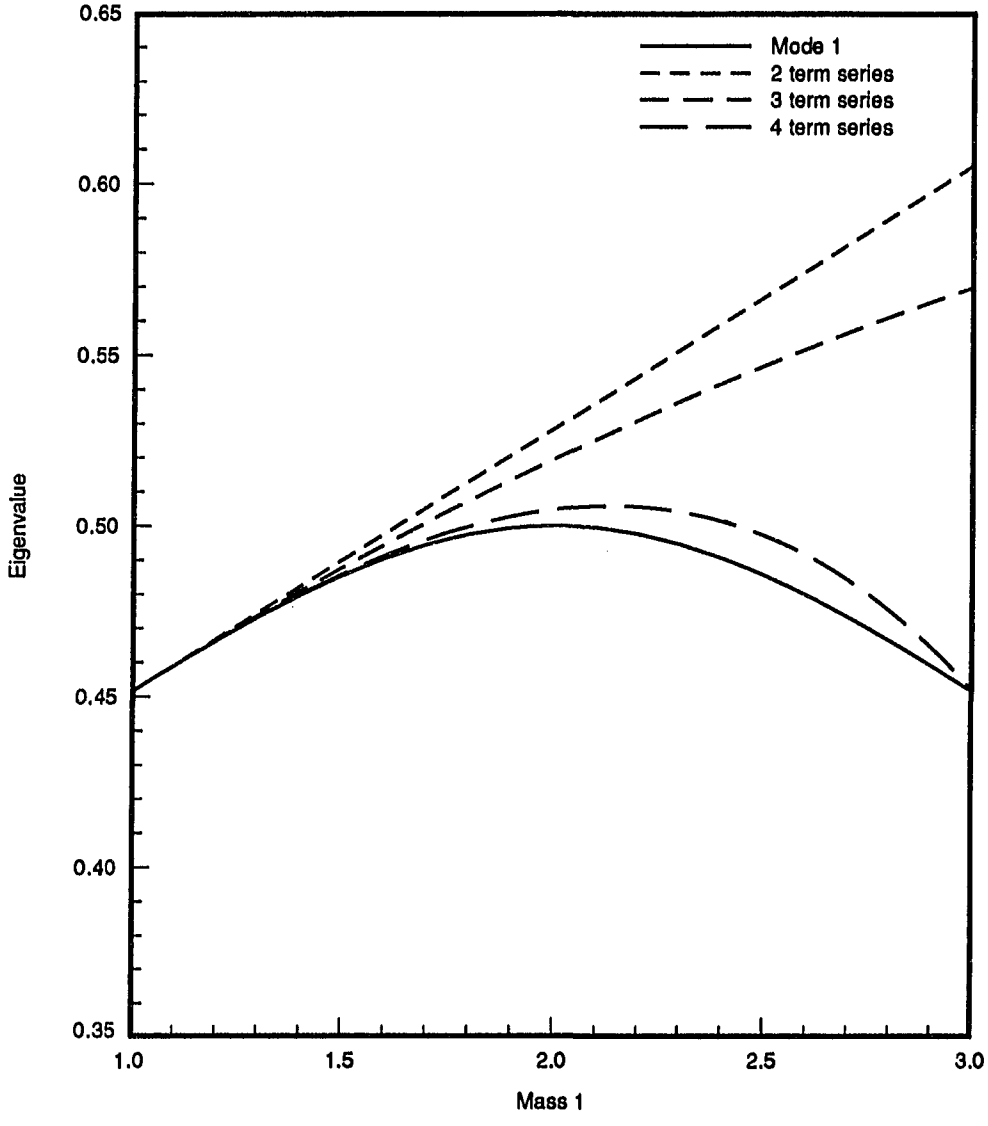

Figure 4.2: Mode 1 power series approximation (up to 4 terms)

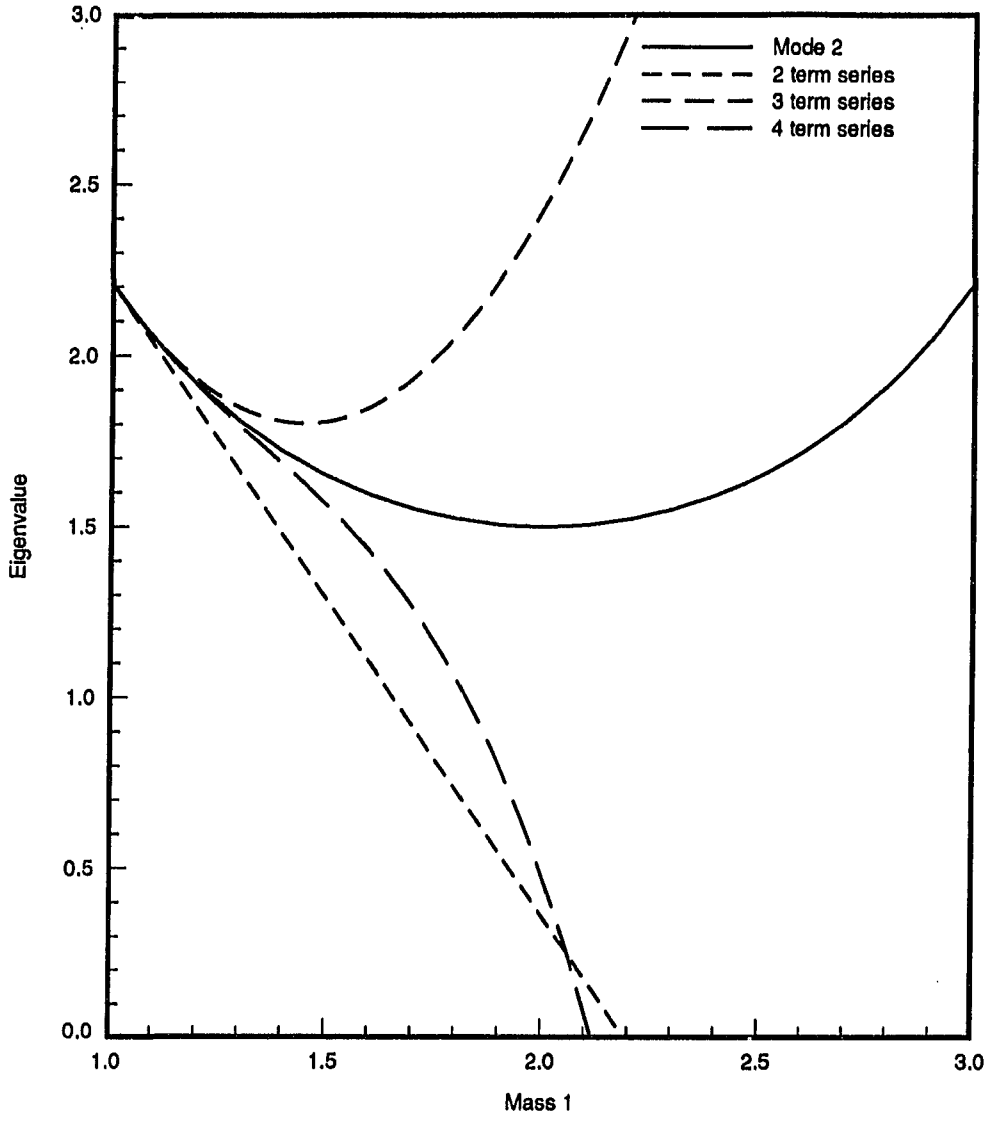

Figure 4.3: Mode 2 power series approximation (up to 4 terms)

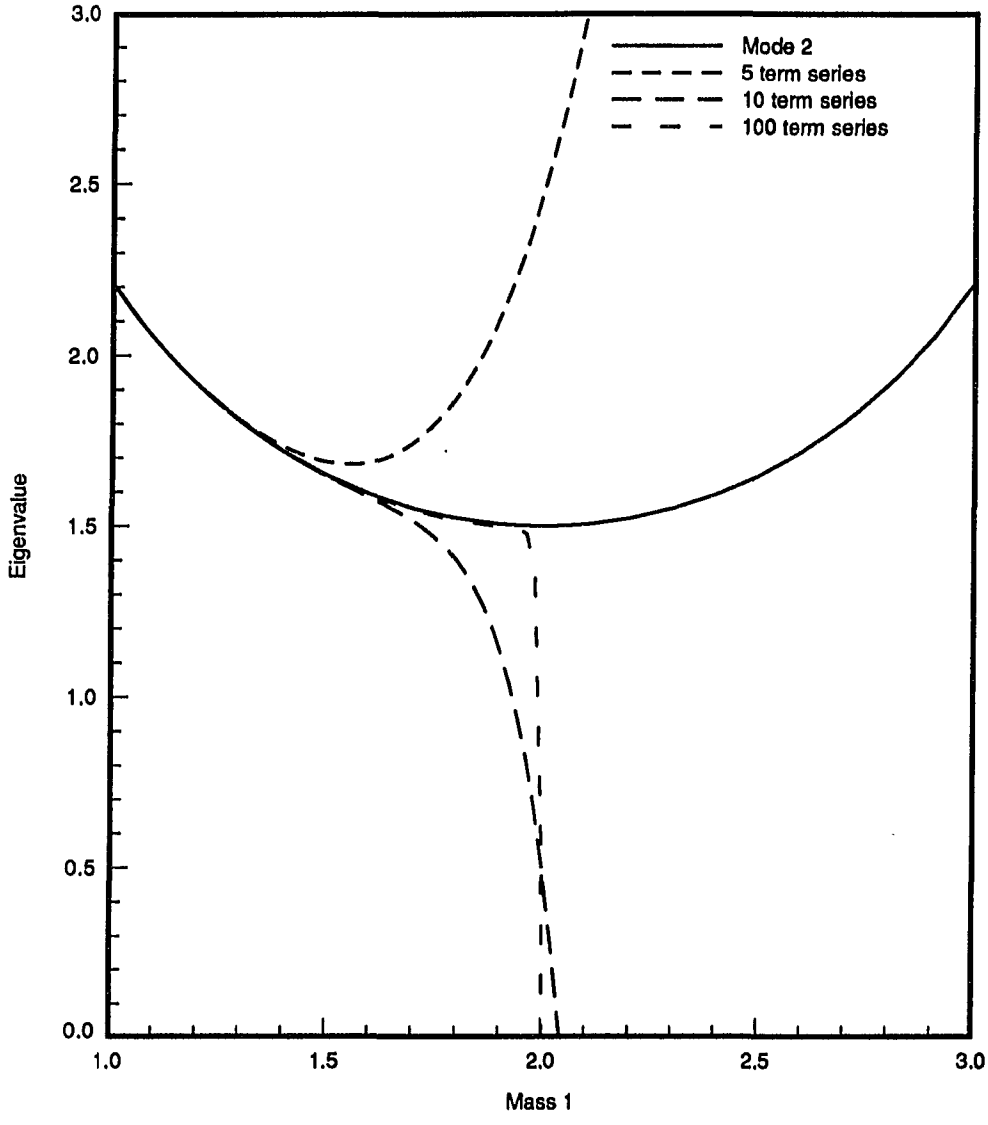

Figure 4.4: Mode 2 power series approximation (up to 100 terms)

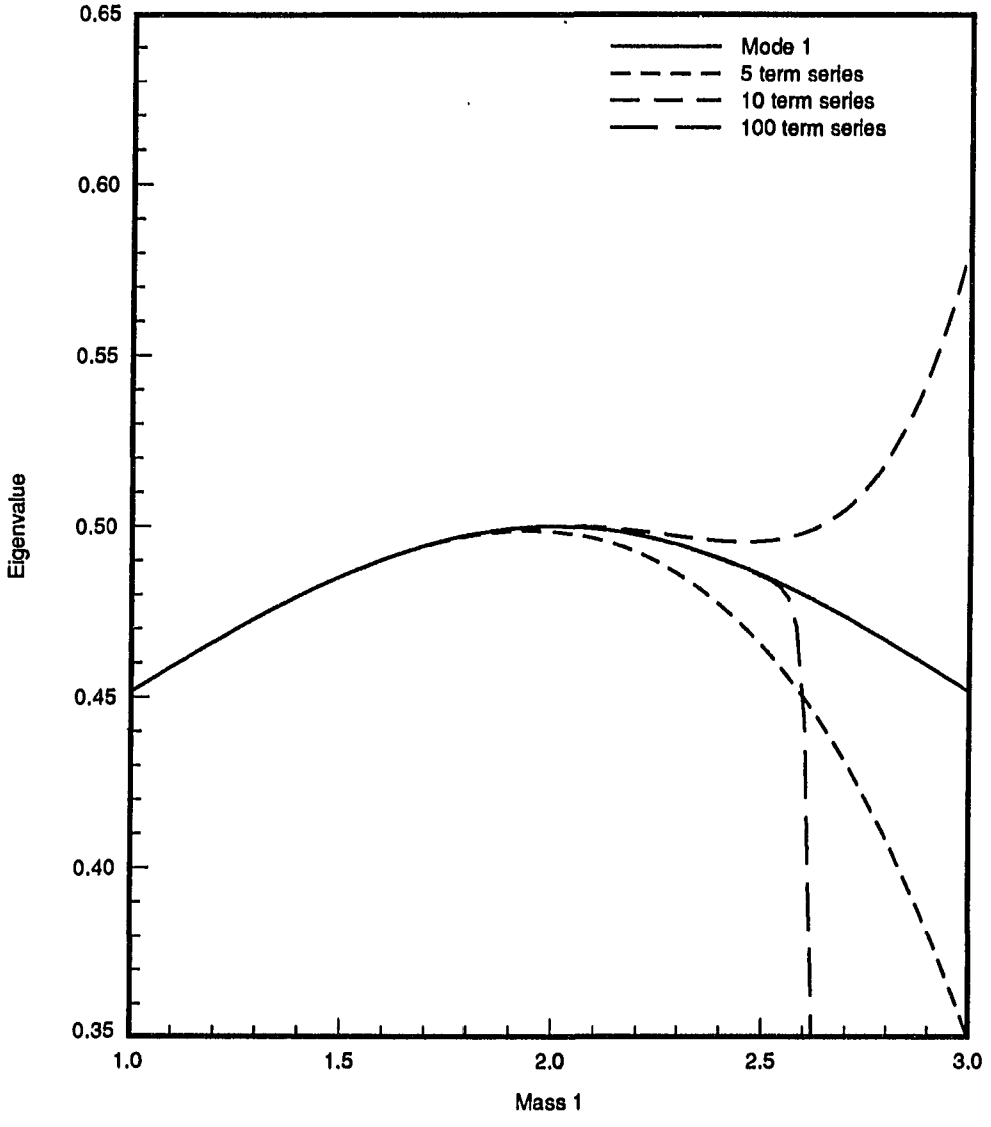

Figure 4.5: Mode 1 power series approximation (up to 100 terms)

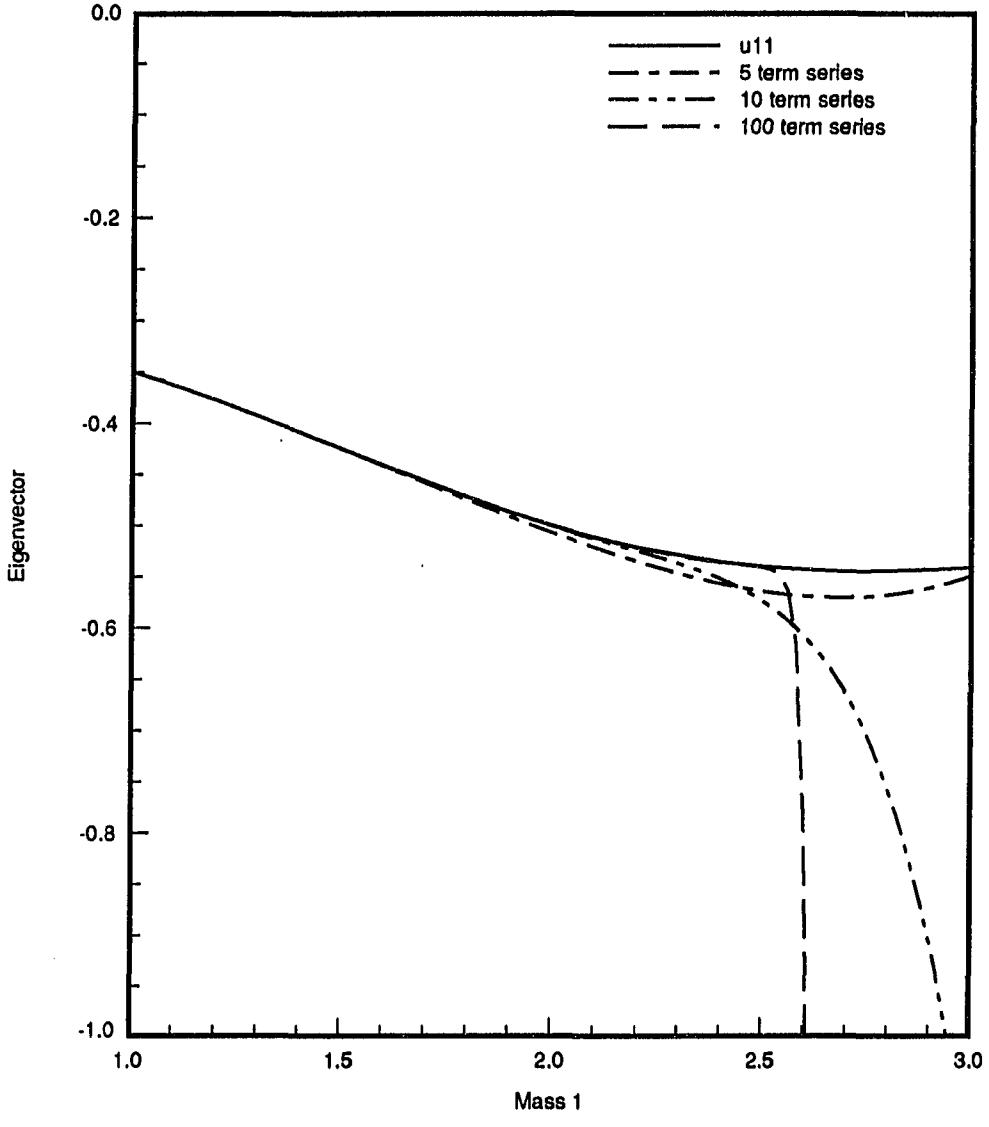

Figure 4.6: Mode 1 power series approximation of eigenvector $u11$

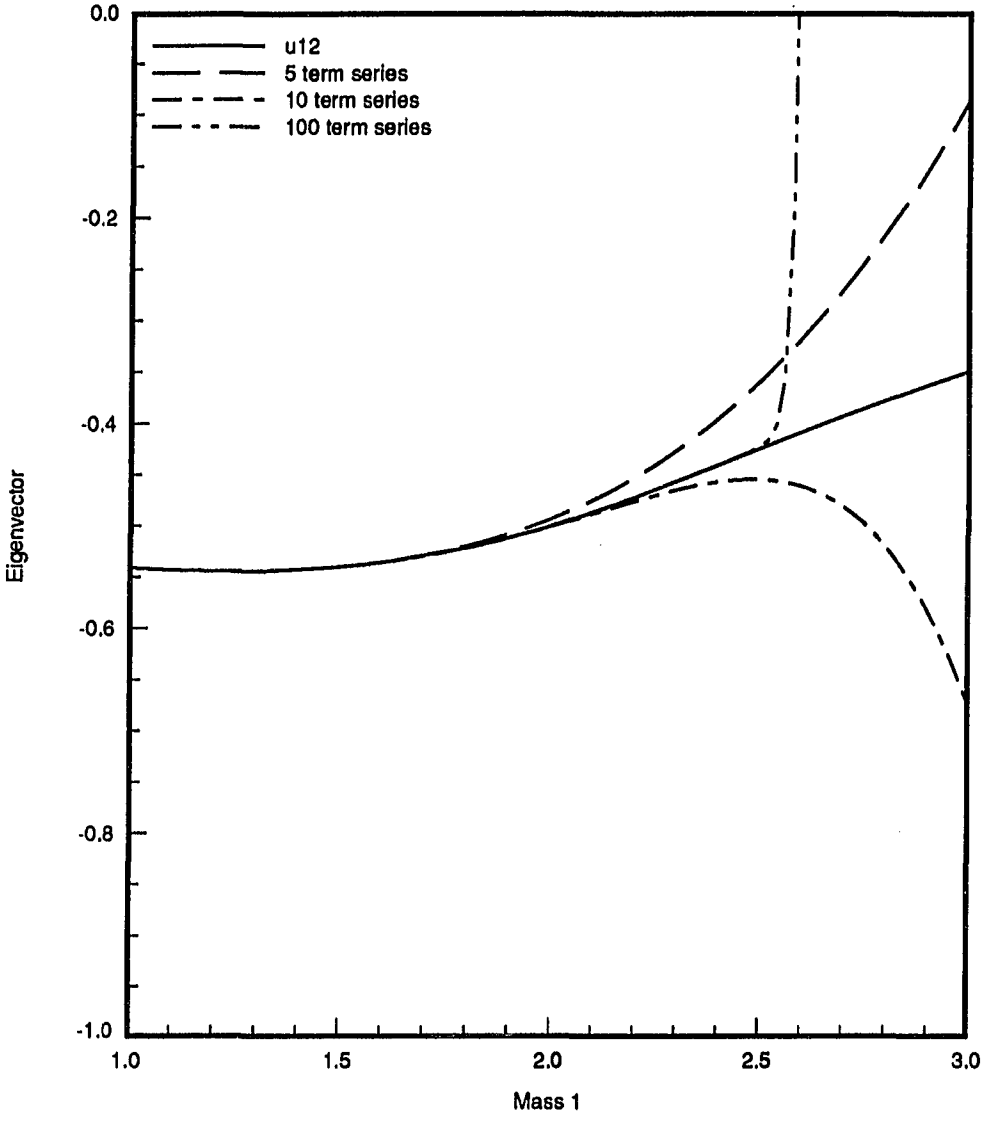

Figure 4.7: Mode 1 power series approximation of eigenvector $u12$

series again diverges at $m1 \approx 2.6$.

Figures 4.8 and 4.9 show approximations for the eigenvector entries for mode 2. Here the series again appears to diverge at $m1 \approx 2.0$.

Padé Approximants of Eigenvalues

Whitesell[26] used Padé Approximants to extend the eigenvalue approximation beyond the poles of the power series. The Padé approximant $R_{l,m}$ for a function F, is a ratio of two polynomial functions, P of degree l, and Q of degree m:

$$R_{l,m} = P_l/Q_m \tag{4.1}$$

To form the Padé approximant $R_{l,m}$, $l+m+1$ coefficients of the series expression for F are needed. For example, the $R_{3,3}$ Padé, requires seven coefficients, which includes six derivatives and one function evaluation.

One characteristic of Padé approximates is that they will converge to the exact value of the function, F, if the function is a rational function. Kwon and Bernard [27] investigated using the Padé approximant to estimate displacement in the statics problem of the form

$$K(e)x(e) = f(e) \tag{4.2}$$

where K is the stiffness matrix, x is the displacement vector, f is the applied force, and e is the design variable. They replaced each element in the K matrix with a cubic polynomial in e resulting in a new set of equations. The solution to the new set of equations, x_{est}, is a rational function of the design variable. Therefore the Padé approximant converged to the exact solution of the new problem.

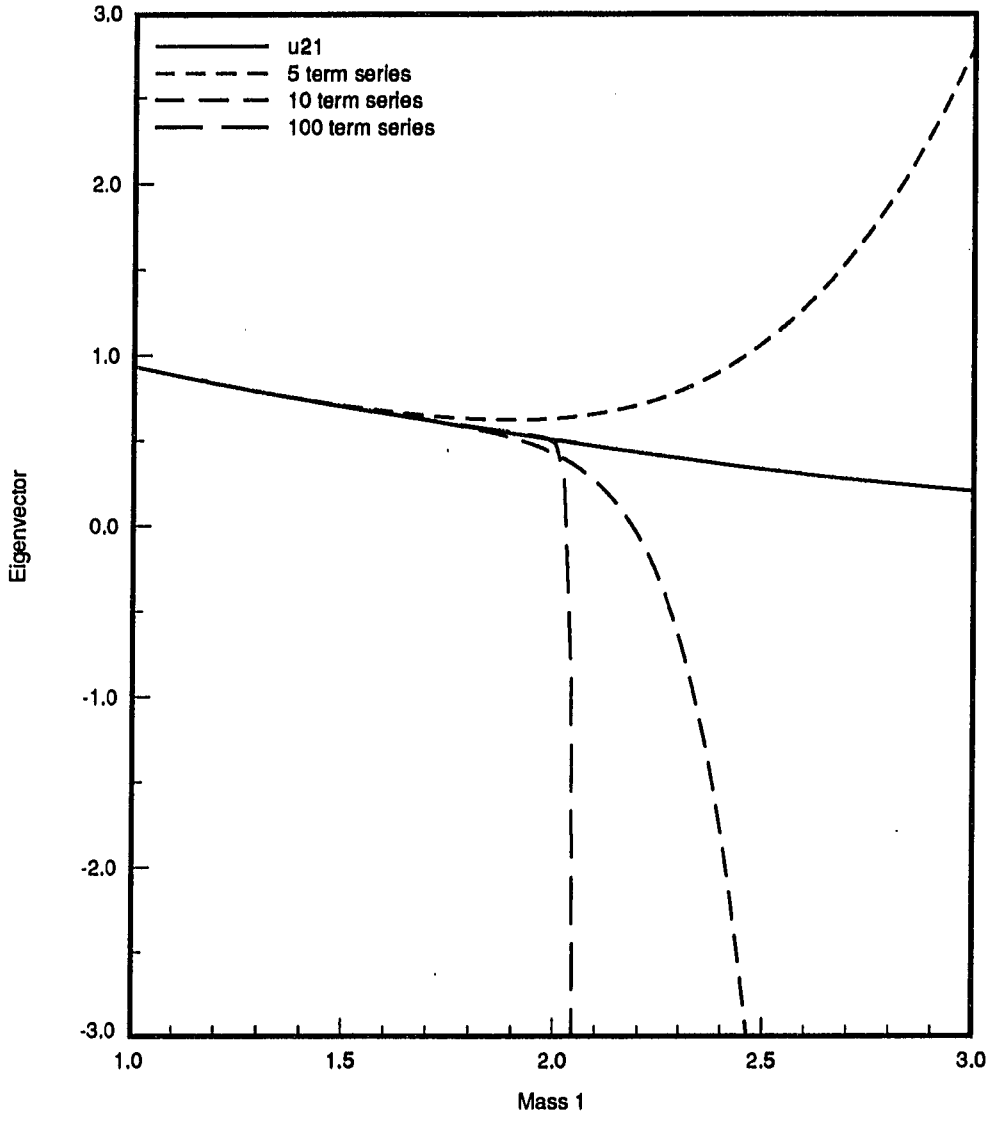

Figure 4.8: Mode 2 power series approximation of eigenvector $u21$

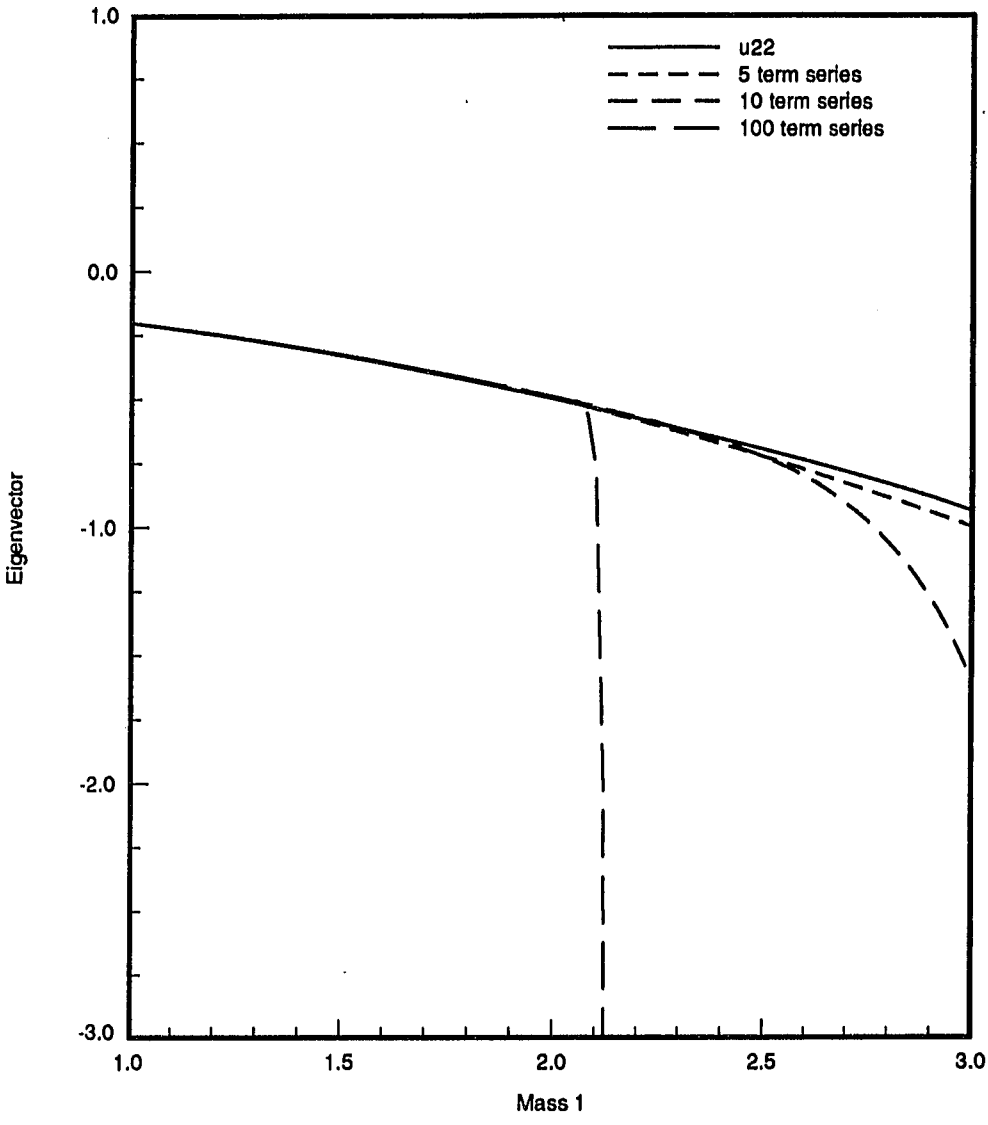

Figure 4.9: Mode 2 power series approximation of eigenvector $u22$

For the eigenvalue problem of equation (2.1), however, the solution is not generally a rational function. The solution is obtained by finding the roots of an n^{th} order polynomial in λ. In that case, the convergence of the Padé is not guaranteed. Numerical results presented here do, however, indicate improvements over the Taylor series approximation.

Figure 4.10 shows the mode 1 Padé approximants from $R_{3,3}$ to $R_{8,8}$, of the eigenvalues across the design range from $m1 = 1.0$ to $m1 = 3.0$. Although the range of validity of the approximation has been extended beyond that obtained using the power series, problems occur near the far end of the design range.

Figure 4.11 shows the Padé approximants for the mode 2 eigenvalues. Similar to mode 1, the range of validity has been extended beyond the Taylor series, but the fit does not satisfactorily cover the entire range.

Curve Fit Approximations of Eigenvalues and Eigenvectors

Although the Padé approximants extend the valid range of the approximations beyond the power series approximations, it is apparent from Figures 4.10 and 4.11 that convergence across the entire design range is not guaranteed.

An approach to resolving this difficulty is to use curve fit techniques across a given design range. These techniques require another solution at the far end of the design space, but force the approximation to match the correct solution at the end of the range. For example, a cubic curve fit across the design range can be computed using the eigensolution and the first derivatives at each endpoint of the design range. For a fifth-order curve fit, additional information might include the second derivatives at each end of the design range.

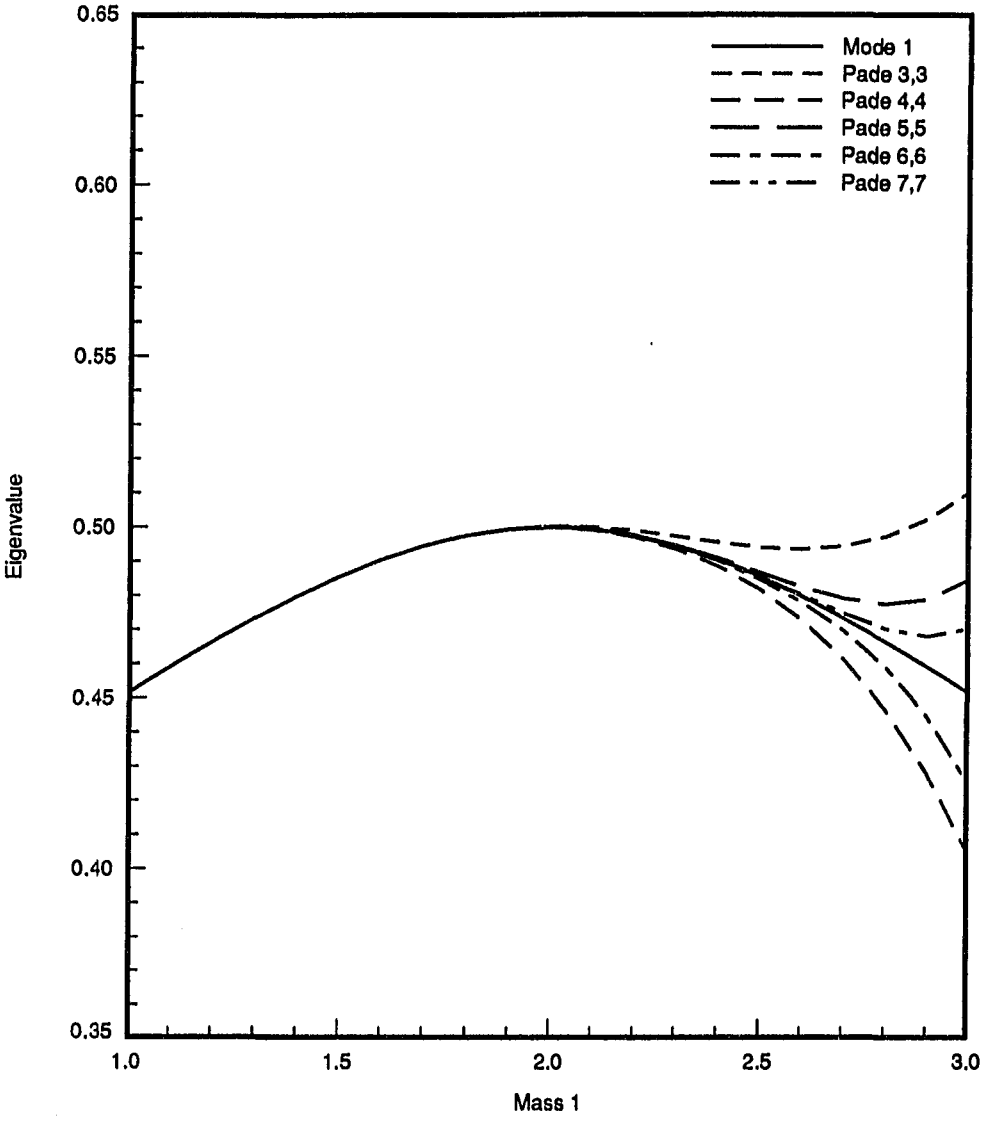

Figure 4.10: Mode 1 Padé approximation

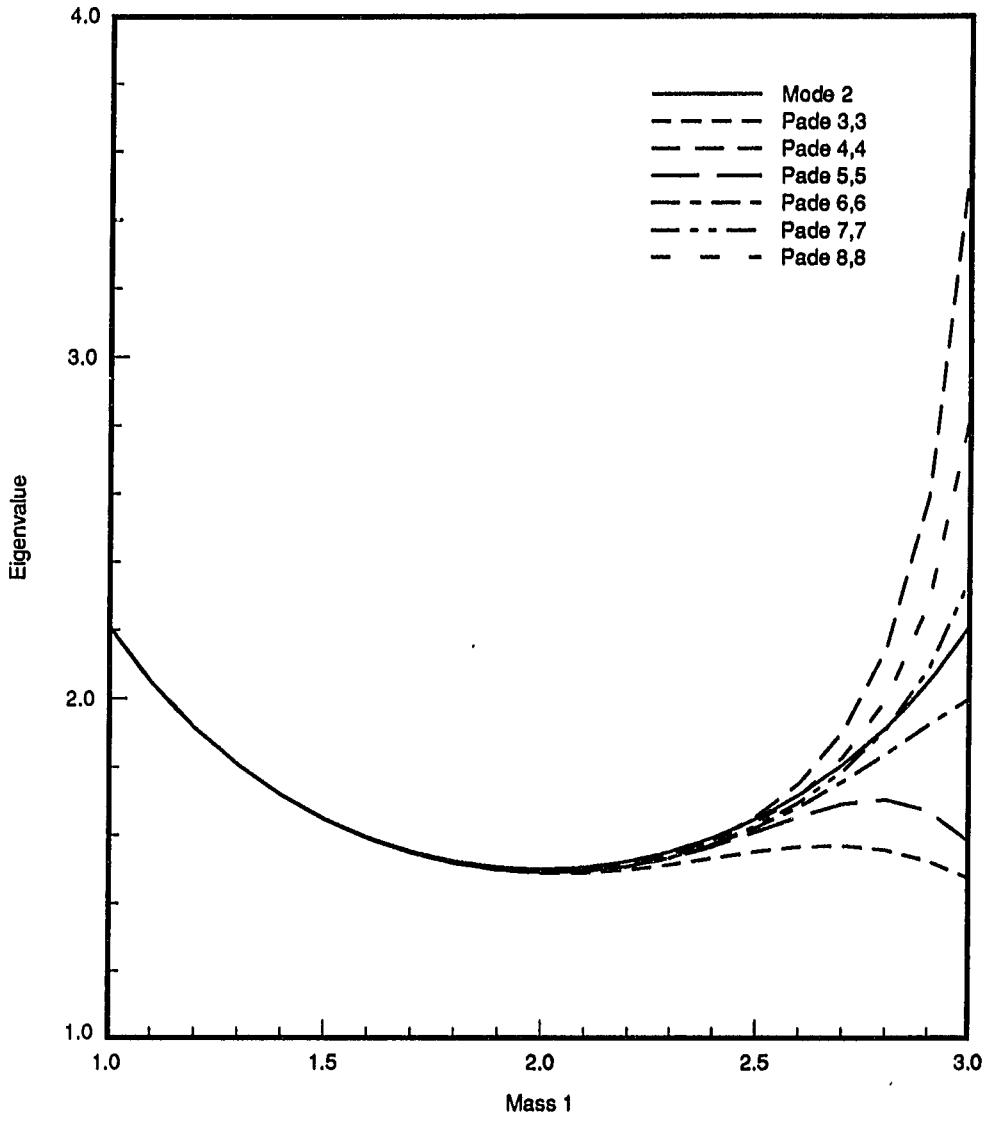

Figure 4.11: Mode 2 Padé approximation

Figure 4.12 shows both a cubic curve fit and a fifth-order curve fit for the eigenvalues of mode 1. Figure 4.13 shows both a cubic curve fit and a fifth-order curve fit for mode 2. For both modes the fifth-order fit resulted in a fairly good approximation across the range. Similar results were found by Vance and Bernard [28] which indicated a fifth-order fit to be a good fit for natural frequencies across a wide range of design variables.

Implementation of the curve fit method faces two challenges. First is the need to identify which eigenvalue at the end of the design range corresponds to the eigenvalue of interest at the beginning of the design range. In modes where the eigenvalues are closely spaced, there is the possibility that multiple roots occur within the design range, resulting in a reordered set of eigenvalues in the part of the range following the multiple root. The second challenge, shared by the power series and Padé methods, is the determination of the margin of error in the approximation at interior points in the design range. The following sections address both of these challenges.

Using the Inner Product to Identify Eigenvalue Match

If curve fits are to be used between re-solve points, a method is needed to identify which eigenvalue at the endpoint of the curve fit corresponds to the eigenvalue of interest at the beginning of the curve fit. The method presented here takes advantage of the fact that eigenvectors are orthogonal with respect to the mass matrix if the corresponding eigenvalues are distinct.

This relationship can be written:

$$U_m^T M U_p = \left\{ \begin{array}{ll} \delta & for\ p = m, \\ 0.0 & for\ p \neq m \end{array} \right\} \tag{4.3}$$

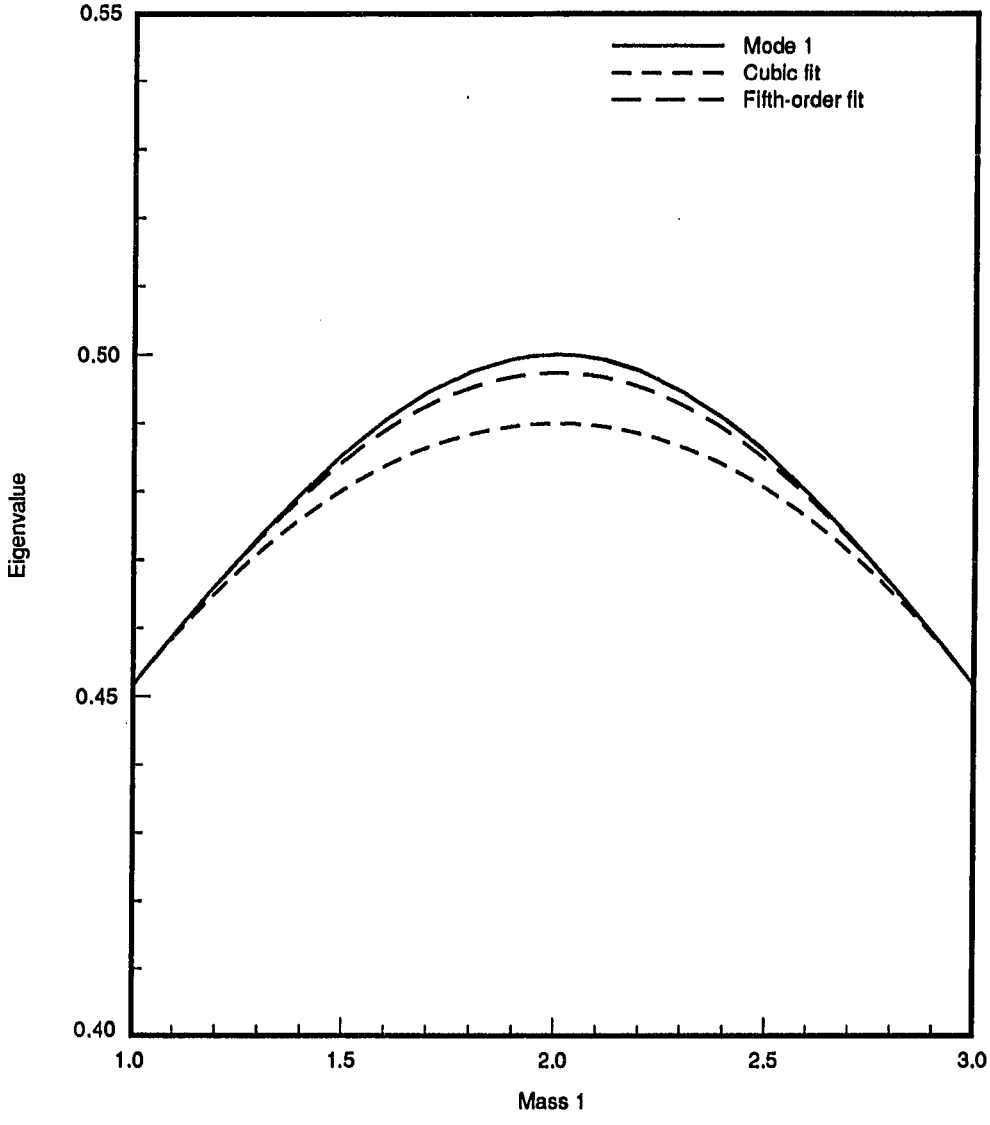

Figure 4.12: Mode 1 cubic and fifth-order approximations

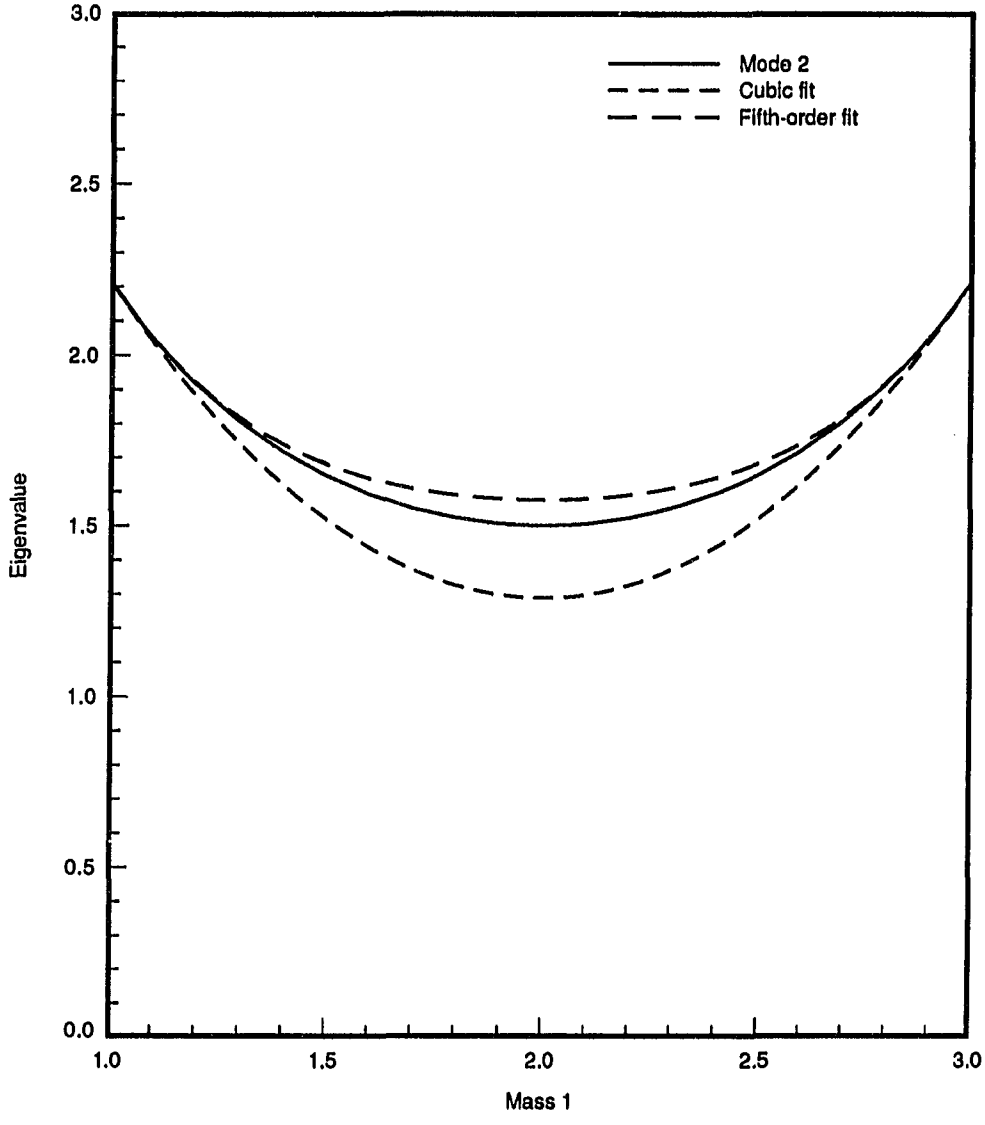

Figure 4.13: Mode 2 cubic and fifth-order approximations

where δ is any scalar quantity. It is common to scale the eigenvectors so that $\delta = 1.0$. This relationship can be used to identify the matching eigenvector at the end of the design range.

First a power series or a Padé approximant of the eigenvector, U_m^*, is formed based on an expansion of the solution at the original design value,e_o. Then $(U_m^*)^T M U_p$ can be computed, where M is the mass matrix and U_p are the eigenvectors at the re-solve point. If U_m^* is the matching eigenvector to U_p, for a given p, then the inner product should be close to 1.0 and $(U_m^*)^T M U_p$ should be close to 0.0 for all other values of p.

In addition to identifying which set of eigenvalues and eigenvectors should be used for the curve fit, the inner product matching technique is a further check on the accuracy of the approximation for the eigenvector. If the inner product matching technique indicates that $(U_m^*)^T M U_p$ is not close to 1.0 for any U_p, then U_m^* is not a good approximation for any of the eigenvectors at that point. If no match is found, the current design range should be reduced until a match can be found.

This approach was applied to the two-degree-of-freedom system of Figure 4.1. A 4-term power series for the eigenvalue is formed based on the eigenvalue at the original design point and its first, second and third derivatives. An estimate of the eigenvector at the end of the design range is made using the series. A solution is obtained at the end of the range where $m1 = 3.0$ and the inner product of $(U_m^*)^T M U_p$ for both modes is shown in Table 4.1.

The procedure is to accept the match when the absolute value of the inner product of $(U_m^*)^T M U_p$ is between 0.9 and 1.1. As can be seen in Table 4.1, an acceptable match has not been found using the 4-term series across the entire design range. This

Table 4.1: Inner product of $(U_m^*)^T MU_p$ for $m1 = 3.0$

Inner product with	MU_1	MU_2
U_1^*	1.290	-0.231
U_2^*	-2.906	-0.099

indicates that the series approximation does not provide a good approximation for either of the eigenvectors at $m1 = 3.0$.

The next step is to divide the design range in half and look at the inner product there to see if a match can be identified. Table 4.2 presents the results of the inner product at $m1 = 2.0$.

Table 4.2: Inner product of $(U_m^*)^T MU_p$ for $m1 = 2.0$

Inner product with	MU_1	MU_2
U_1^*	1.022	0.017
U_2^*	0.151	0.862

These results indicate that U_1 at the original design point matches with U_1 at $m1 = 2.0$. Since there are only two modes, U_2 at the original design point must match with U_2 at $m1 = 2.0$. The second half of the range from $m1 = 2.0$ to $m1 = 3.0$ is investigated in the same manner.

Once the matches are determined, curve fits are calculated. Since three derivatives are available at each end of the range, a seventh-order curve fit can be used. Figures 4.14 and 4.15 present the approximation of the eigenvalues across the entire design range using a seventh-order curve fit between $m1 = 1.0$ and $m1 = 2.0$ and another seventh-order fit between $m1 = 2.0$ and $m1 = 3.0$.

Figures 4.16 and 4.17 show the approximation of the eigenvectors across the entire design range using similar seventh-order fits.

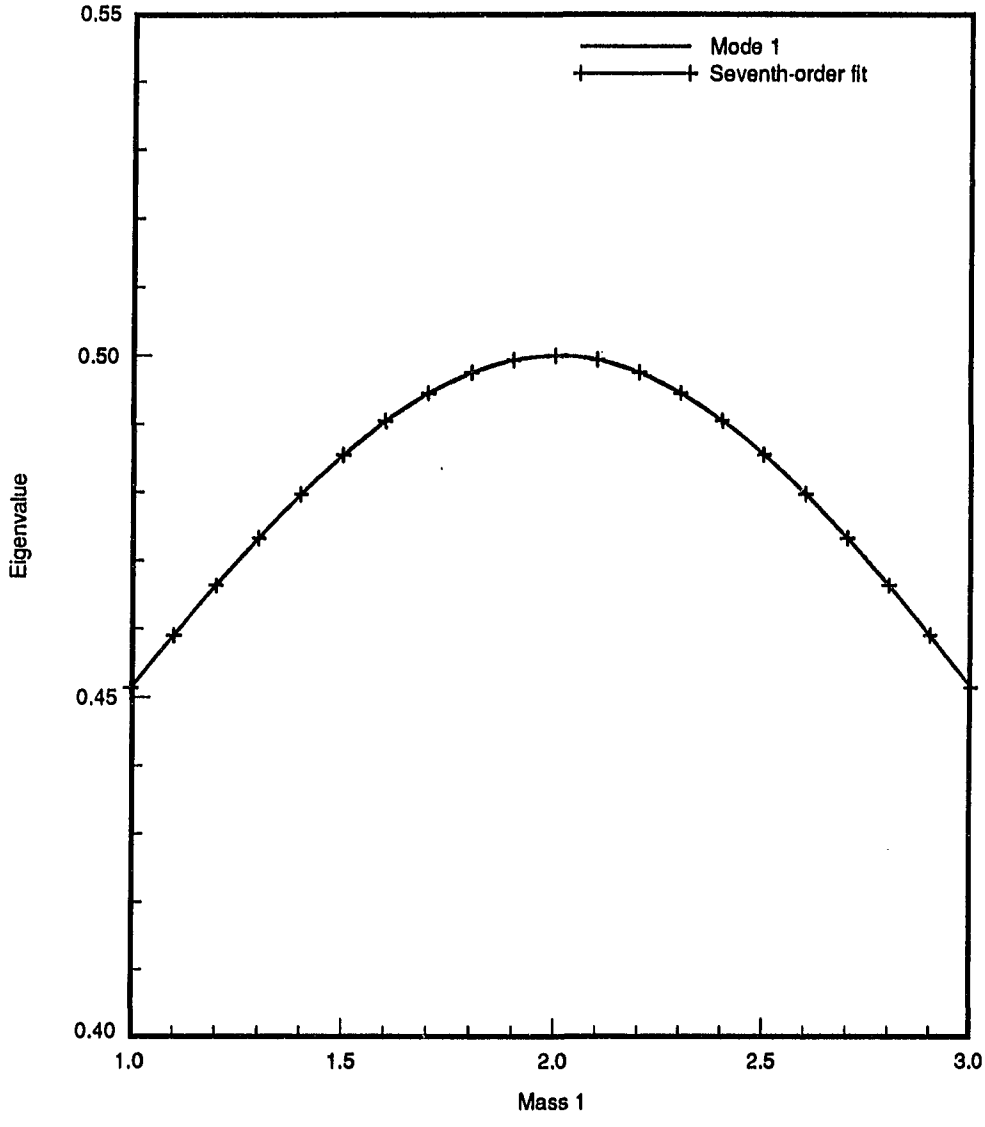

Figure 4.14: Mode 1 eigenvalue approximation using inner product matching: re-solve at $m1 = 2.0$

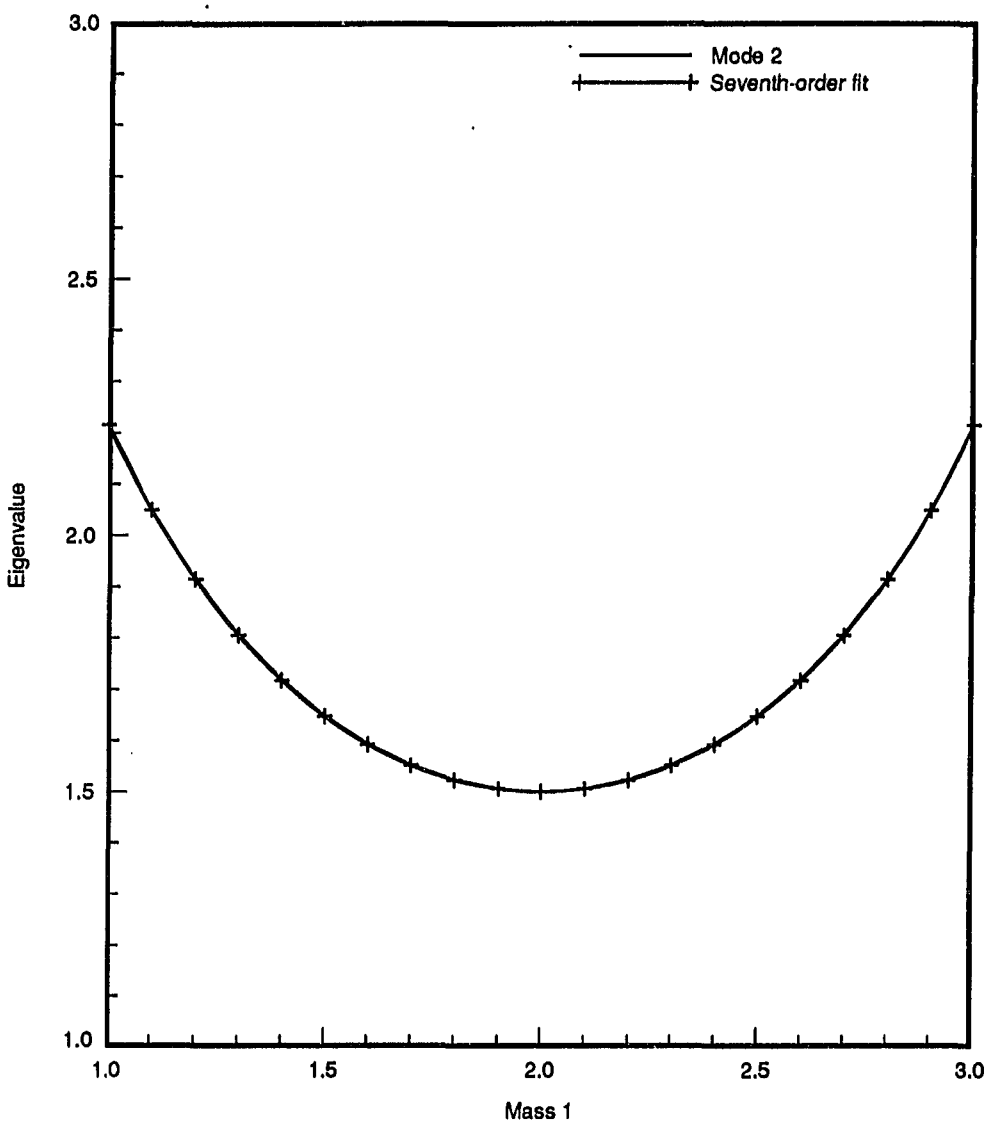

Figure 4.15: Mode 2 eigenvalue approximation using inner product matching: re-solve at $m1 = 2.0$

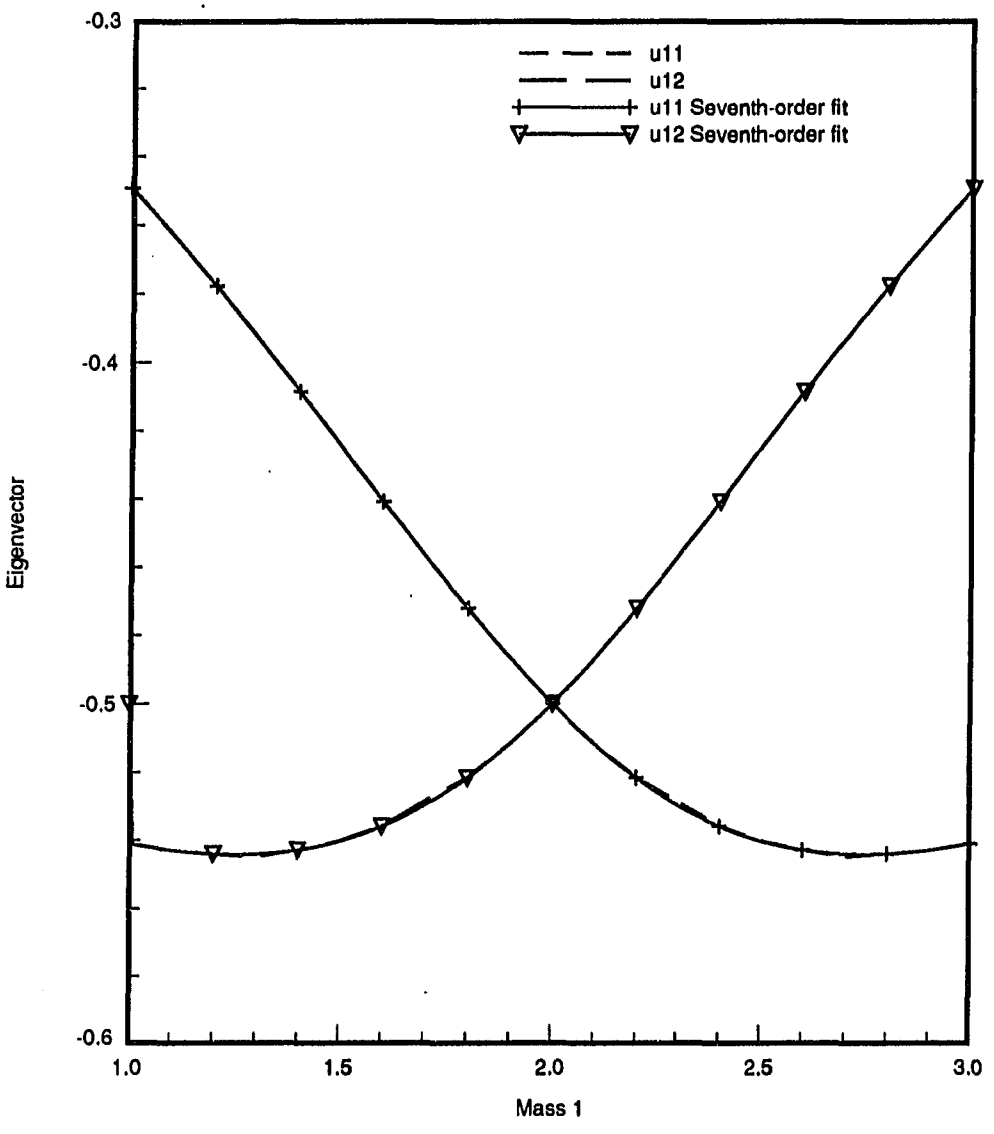

Figure 4.16: Mode 1 eigenvector approximation using inner product matching: re-solve at $m1 = 2.0$

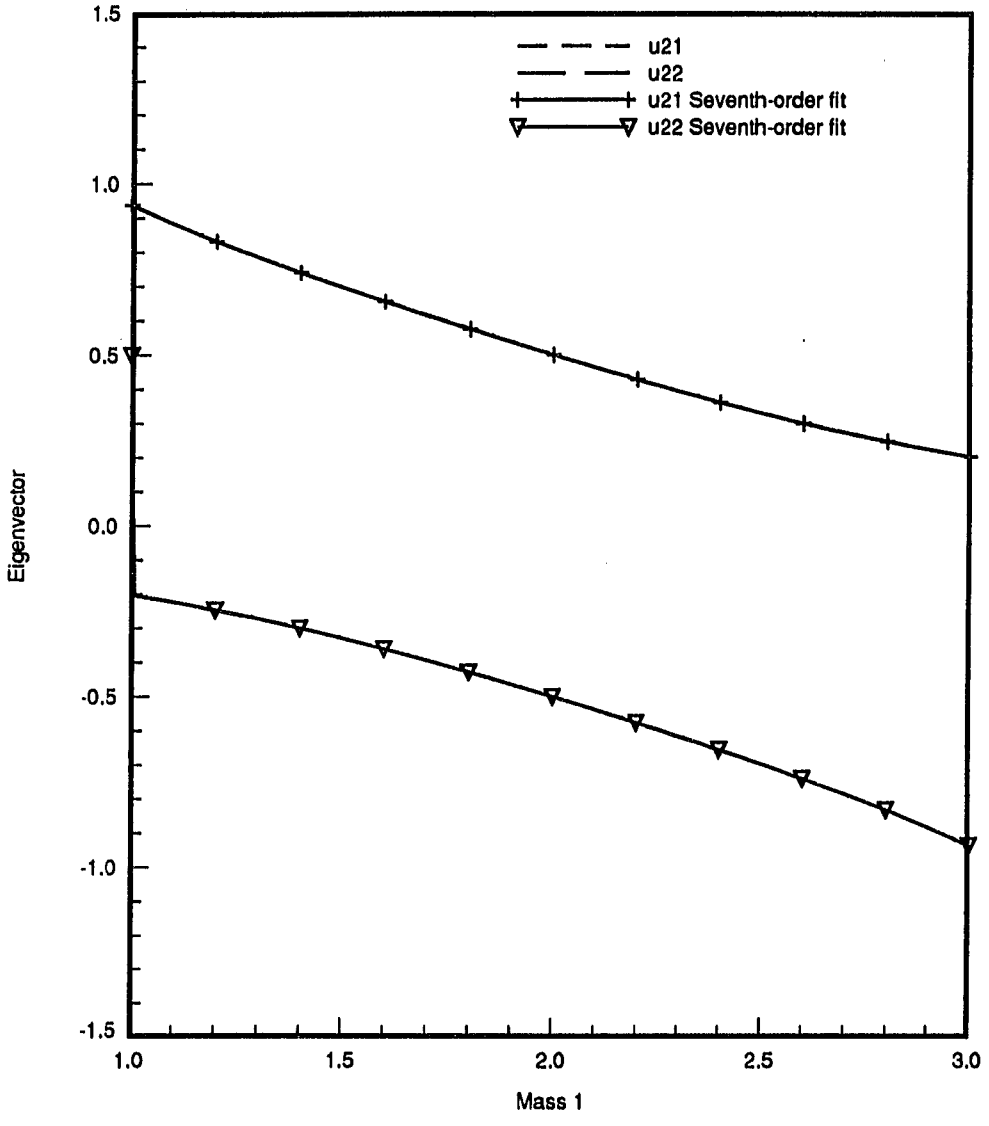

Figure 4.17: Mode 2 eigenvector approximation using inner product matching: re-solve at $m1 = 2.0$

Using Cut Off Percents to Determine When to Re-solve

A major challenge encountered when trying to use either Taylor series or Padé approximants to estimate eigenvalues or eigenvectors is determining when the approximation is beginning to diverge. In a power series, an indication that the series is beginning to loose accuracy is when the addition of one more term causes the approximation to vary widely from the previous approximation. Therefore, to determine when the series is starting to diverge, the series value can be compared to the value resulting from adding one more term to the series. If the absolute value of the additional term series is greater than a certain percent of the current approximation then divergence is indicated and a re-solve is needed. At the point of the re-solve, new derivatives can be calculated and a new power series could be formed to continue the approximation across the design range. A similar method can be used to determine when the Padé approximant is starting to diverge.

Either the power series or the Padé approximant could be used to provide estimated eigenvalues and eigenvectors for the range between the re-solve points, however, since derivatives are calculated at the re-solve point, forming a curve fit between re-solve values would further improve the accuracy of the approximation in the range around the re-solve value.

The approach taken was to approximate eigenvalues with a power series or a Padé approximant, checking at each change in design for an indication of divergence of the series. When the need for a re-solve is indicated, new derivatives are calculated at that point to be used in further projections forward across the design space. These derivatives are also used as endpoint values for forming a curve fit back to the previous solution. The curve fit is used for the approximation of the eigenvalues within the

area of the design range between re-solves. Inner product matching is also used to identify the matching eigenvalues and eigenvectors for the curve fit. This procedure was used on the two degree-of-freedom system and values of percent cut off were varied from 2% to 10%.

In making a comparison of approximations based on power series and approximations based on Padé approximants, the comparison should be made between methods requiring the same number of derivatives. For example, an n-term power series requires $n-1$ derivatives. For an $R_{l,m}$ Padé, $l+m$ derivatives are needed. Therefore an 9-term power series requires the same number of derivatives as an $R_{4,4}$ Padé approximant.

Table 4.3 lists the number of re-solves needed to span the design space for mode 1, and Table 4.4 lists the same information for mode 2. The number of re-solves shown in the tables includes one re-solve at the end of the design range for each method. The $R_{3,3}$ and $R_{4,4}$ were used because they are the lowest Padé approximants that would give convergence. The 9-term power series was included because that series requires the same number of derivatives as the $R_{4,4}$.

Table 4.3: Mode 1: Number of re-solves needed for solution

Percent cut off	2-term/3-term	3-term/4-term	8-term/9-term	$R_{3,3}/R_{4,4}$
2%	3	3	3	3
5%	3	2	2	3
10%	2	3	2	3

Table 4.5 shows the value of $m1$ at each re-solve for mode 1 using a cut off of 2% and inner product matching in the range of 0.9 to 1.1. Table 4.6 shows the corresponding information for mode 2. The parentheses show where the inner product matching could not find a match for the previous value of $m1$ in the table. In that

case the current range was reduced by half and a match was found at the value of $m1$ shown in parentheses.

Table 4.4: Mode 2: Number of re-solves needed for solution

Percent cut off	2-term/3-term	3-term/4-term	8-term/9-term	$R_{3,3}/R_{4,4}$
2%	10	5	3	2
5%	7	3	2	2
10%	5	4	2	2

Table 4.5: Mode 1: $m1$ values resulting from 2% cut off re-solve criterion

2-term/3-term	3-term/4-term	8-term/9-term	$R_{3,3}/R_{4,4}$
2.10	1.89	2.84	2.46
2.51	2.92	(1.92)	(1.73)
3.00	3.00	3.00	3.00

Table 4.6: Mode 2: $m1$ values resulting from 2% cut off re-solve criterion

2-term/3-term	3-term/4-term	8-term/9-term	$R_{3,3}/R_{4,4}$
1.14	1.27	1.63	2.32
1.30	1.63	2.74	3.00
1.48	2.17	3.00	xxxx
1.69	2.99	xxxx	xxxx
1.91	3.00	xxxx	xxxx
2.14	xxxx	xxxx	xxxx
2.38	xxxx	xxxx	xxxx
2.61	xxxx	xxxx	xxxx
2.82	xxxx	xxxx	xxxx
3.00	xxxx	xxxx	xxxx

As indicated in Table 4.5, for mode 1 there are three curve fits needed for the 2-term/3-term series: from $m1 = 1.00$ to 2.10, from $m1 = 2.10$ to 2.51, and from $m1 = 2.51$ to 3.00. This requires re-solves and derivative calculations at $m1 = 2.10$,

2.51, and 3.00. The required calculations for the 3-term/4-term series are similar, with curve fits from $m1$ = 1.00 to 1.89, 1.89 to 2.92, and 2.92 to 3.00.

Using the 8-term/9-term series results in two curve fits across the range: from $m1$ = 1.00 to 1.92 and from $m1$ = 1.92 to 3.00. The first re-solve indicated by the cut off percent was at $m1$ = 2.84 where an additional solution was obtained. While the cut off percents indicated that the 8-term/9-term series remained accurate over a wide range of design changes, the inner product matching indicated that the approximation of the eigenvector at $m1$ = 2.84 was not close to either of the actual eigenvectors. Therefore the range was reduced and inner product matching performed again. Similarly, the $R_{3,3}/R_{4,4}$ Padé requires only two curves to fit the range: from $m1$ = 1.00 to 1.73 and from $m1$ = 1.73 to 3.00, but an additional solution was calculated at $m1$ = 2.46.

When considering the number of terms to use in the curve fit, it is generally the case that the cost of calculating the curve fit is significantly smaller than the cost of calculating the derivatives. So using all of the available derivatives in the curve fit is economical. For the 2-term/3-term series, two derivatives at each end of the range and two function solutions are available so a fifth-order curve fit can be used between the re-solve values. Similarly, for the 3-term/4-term series, a seventh-order curve fit can be used. For both the 8-term/9-term series and the $R_{3,3}/R_{4,4}$ Padé, eight derivatives at each end of the range and two function values are available. Theoretically a 17^{th} order curve fit could be used. In practice, however, numerical errors were encountered when trying to obtain the coefficients of the blending functions needed for the 17^{th} order curve fit. Using three derivatives at each end of the range and the two function solutions allowed for a seventh-order curve fit and numerical errors were

not encountered.

Figure 4.18 shows a fifth-order fit between the re-solve points for the 2-term/3-term series and seventh-order fits for the 3-term/4-term series, 8-term/9-term series and the Padé approximation.

Used in a design process, these methods present trade-offs between the cost of calculating the number of derivatives required for the fit and the cost of each re-solve. Table 4.6 shows that when comparing the 2-term/3-term series to the 3-term/4-term series, the 3-term/4-term series requires fewer re-solves for the cost of just one more derivative calculation. If one derivative calculation was less expensive than five re-solves, the 3-term/4-term method would be preferred.

For the additional calculation of five more derivatives, the 8-term/9-term series can reduce the number of re-solves from those required for the 3-term/4-term for mode 2. However, using the same number of derivative calculations, the $R_{4,4}$ can further reduce the number of re-solves needed. If eight derivatives are used, the $R_{3,3}/R_{4,4}$ can provide an approximation across the space using three fewer re-solves than the 8-term/9-term series. If the cost of calculating five derivatives is less expensive than a re-solve, then the $R_{3,3}/R_{4,4}$ method would be preferred for mode 2.

In this way, the choice between using a Taylor series or a Padé approximant method is problem dependent and related to the relative cost of calculating derivatives and re-solving the system equations. The one observation that can be made is that when the Padé approximant is compared to a power series of the same order, the Padé can generally approximate the function for larger design changes before divergence is detected.

The next chapter applies these methods to a larger finite element-based problem.

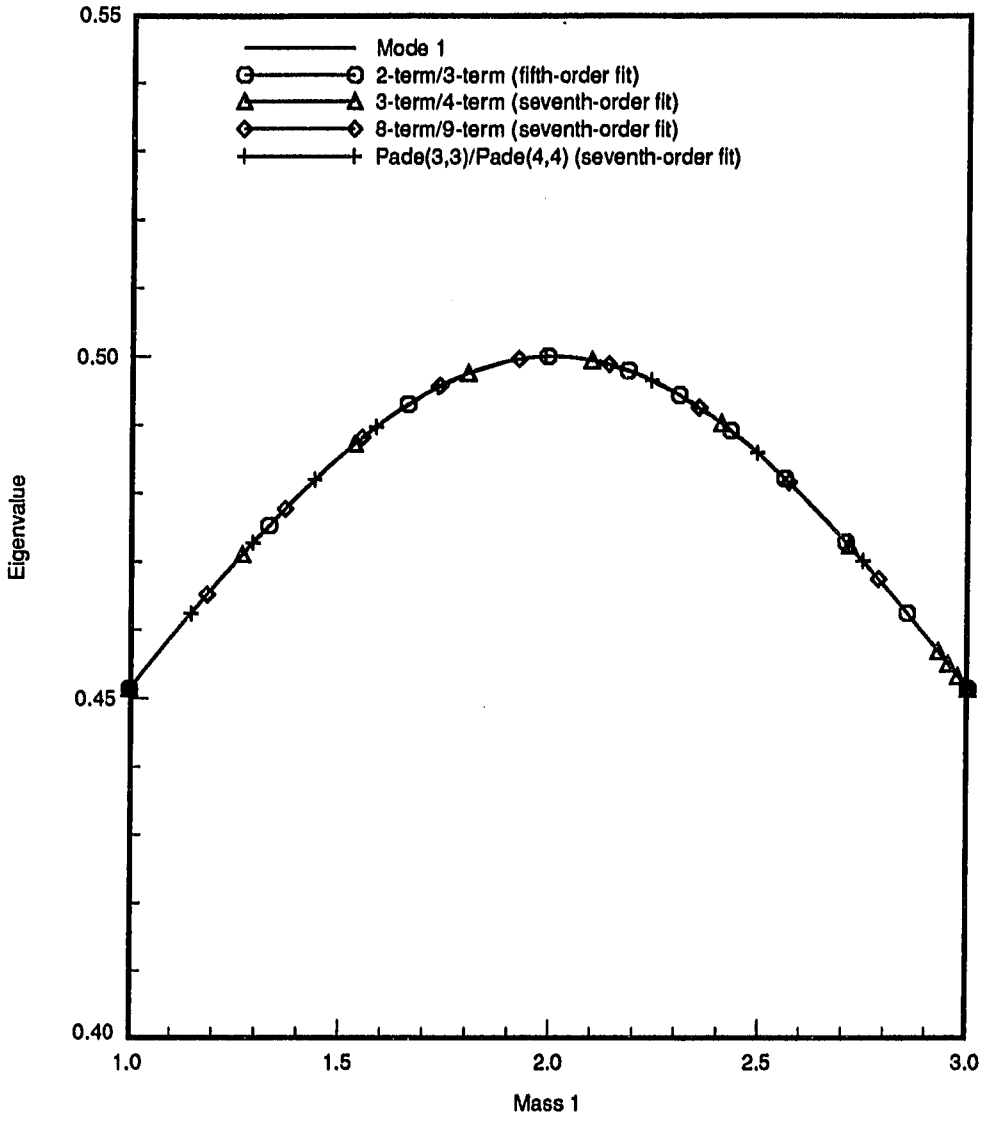

Figure 4.18: Mode 1 curve fit between re-solve points: using inner product matching

CHAPTER 5. FINITE ELEMENT MODEL

The methods of power series and Padé approximants combined with curve fits, percent cut offs, and inner product matching which were presented in the previous chapter are applied here to a finite element model. This example approximates the first, second, and ninth eigenvalues and eigenvectors of a plate with respect to a very large change in thickness of one portion of the plate.

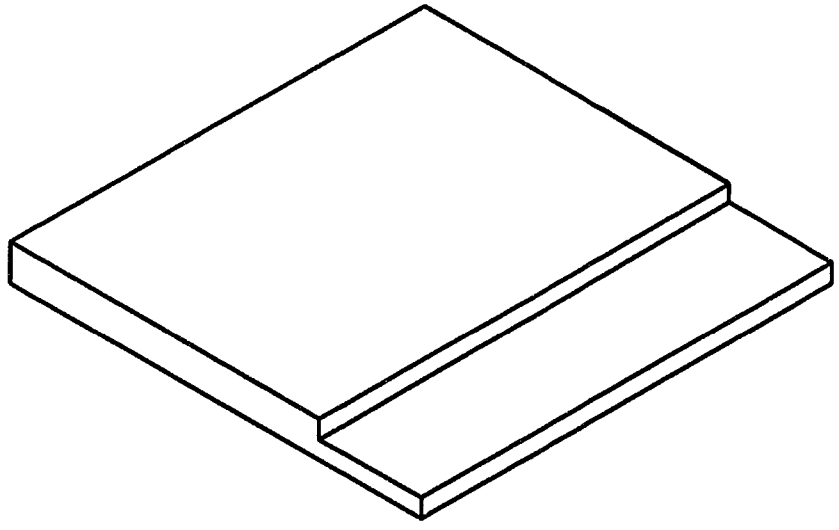

Figure 5.1: The plate model

The model consists of a square plate as shown in Figure 5.1. The plate was modeled using I-DEAS software [32] from the Structural Dynamics Research Corpo-

ration. The finite element model consisted of 16 quadrilateral shell elements each with 8 nodes. The edges of the plate were fixed, along with the out-of-plane rotation of all of the nodes, yielding 165 degrees of freedom. The properties of the plate are listed in Table 5.1.

Table 5.1: Properties for the square plate model

Width	1.00 m
Length	1.00 m
Initial Thickness	1.00 mm
Modulus of Elasticity	2.067 x 10^3 MPa
Density	7.820 x 10^3 kg/m^3
Poisson's ratio	0.29

The design variable, t, was the thickness of a band on the plate that was located along one side as shown in Figure 5.1. The initial thickness of the band was set at 0.50 mm. The acceptable design range was set at 0.50 mm to 1.20 mm. The commercial finite element code MSC/NASTRAN [30] from the MacNeal-Schwendler Corporation was used for the vibration analysis and derivative calculations.

Following the methods outlined in the previous chapter, estimates of mode 1 and mode 2 were computed using the 3-term/4-term Taylor series, the 8-term/9-term series and the $R_{3,3}/R_{4,4}$ Padé approximant. Each method includes inner product matching and re-solve techniques. A 5% cut off value was chosen to signal when a re-solve should be computed. Similarly, an acceptable the inner product matching range was chosen as 0.9 to 1.1.

Power Series Approximations

The following algorithm was used to determine an approximation for the eigenvalues and eigenvectors across the design range from t_0 to t_l using the 3-term/4-term power series approximations.

1. Solve at t_0 to obtain Λ and U. Λ and U are the set of eigenvalues and eigenvectors of interest.

2. Calculate the derivatives of K and M with respect to t at $t = t_0$.

3. Calculate $\lambda_m^{(1)}$, $\lambda_m^{(2)}$, $\lambda_m^{(3)}$ and $U_m^{(1)}$, $U_m^{(2)}$, $U_m^{(3)}$ at t_0.

4. Project the eigenvalue across the range using both a 3-term Taylor series and a 4-term Taylor series.

5. When the 3-term series and the 4-term series differ by 5%, set $t = t_l$ and re-solve to obtain Λ_l, U_l, and M_l.

6. Project the eigenvector across the range using a 4-term Taylor series based at t_0 to get U_m^* at t_l.

7. Form the inner product of $(U_m^*)^T M_l (U_p)_l$ with several eigenvectors at t_l in order to identify the match between eigenvectors at each end of the range.

8. If the absolute value of the inner product of $(U_m^*)^T M_l$ with an eigenvector, $(U_p)_l$, is between 0.9 and 1.1 then select that eigenvector for a seventh-order spline-fit. Go to step 10.

9. If no eigenvector is selected, let $t_l = (t_0 - t_l)/2$ and re-solve. Go to step 7.

10. Calculate $\lambda_p^{(1)}$, $\lambda_p^{(2)}$, $\lambda_p^{(3)}$ and $U_p^{(1)}$, $U_p^{(2)}$, and $U_p^{(3)}$ at t_l.

11. Form a seventh-order fit between $U_m^{(0)}$, $U_m^{(1)}$, $U_m^{(2)}$, $U_m^{(3)}$ at t_0 and $U_p^{(0)}$, $U_p^{(1)}$ $U_p^{(2)}$, and $U_p^{(3)}$ at t_l.

12. Form a seventh-order fit between $\lambda_m^{(0)}$, $\lambda_m^{(1)}$, $\lambda_m^{(2)}$, $\lambda_m^{(3)}$ at t_0 and $\lambda_p^{(0)}$, $\lambda_p^{(1)}$, $\lambda_p^{(2)}$, $\lambda_p^{(3)}$ at t_l.

13. Continue across the design range by setting $t_0 = t_l$. Go to step 2.

Following this algorithm, a 3-term Taylor series and a 4-term Taylor series were formed for the eigenvalue of mode 1 at $t_0 = 0.50\ mm$. The difference between the 3-term and the 4-term Taylor series didn't reach 5% within the acceptable design range of $t = 0.50\ mm$ to $t = 1.20\ mm$. (At the end of the design range the difference between the two approximations was only 1.68%, indicating that a re-solve was not needed within this range.) The 4-term Taylor series approximation of U_1^* was calculated at $t_l = 1.20\ mm$ and the inner product formed to identify the matching eigenvector. For mode 1, using the entire range from 0.50 mm to 1.20 mm resulted in the values for the inner products as shown in Table 5.2.

Table 5.2: Mode 1 inner product of $(U_1^*)^T M U_p$ for $t_l = 1.20\ mm$

Inner product with	$(U_1^*)^T M U_p$
U_1	-0.9609
U_2	-2.3534 x 10^{-14}
U_3	-0.4473
U_4	4.8433 x 10^{-14}
U_5	-9.0329 x 10^{-2}
U_6	-0.2761

The inner product results show that at $t = 1.20\ mm$, the eigenvector match is with the mode 1 eigenvector, U_1. This indicates that a fit can be made between the mode 1 eigenvector at $t = 0.50\ mm$ and the mode 1 eigenvector at $t = 1.20\ mm$.

To form a seventh-order fit between the two design points, three coefficients at each end of the design range were used, therefore, the first, second and third coefficients are computed at $t = 1.20\ mm$. Figure 5.2 shows the results of the eigenvalue fit across the range.

For mode 2, derivatives are computed at $t = 0.50\ mm$ and the 3-term and 4-term series are formed. A comparison of the two series, indicates that they differ by 5% at $t = 0.776\ mm$. This indicates that a re-solve is needed at this point. A re-solve is performed and M, Λ and U at $t = 0.776\ mm$ are obtained. The derivatives of M and K are also re-computed at $t = 0.776\ mm$. Next, an estimate of the eigenvector at $t = 0.776\ mm$, U_2^*, is made using the 4-term series, and the inner product with $(U_2^*)^T M U_p$ at $t = 0.776\ mm$ is computed. The results of the inner product calculation are shown in Table 5.3.

Table 5.3: Mode 2 inner product of $(U_2^*)^T M U_p$ for $t_l = 0.776\ mm$

Inner product with	$(U_2^*)^T M U_p$
U_1	-2.3282 x 10^{-2}
U_2	-0.9944
U_3	5.3469 x 10^{-13}
U_4	-8.9373 x 10^{-15}
U_5	-9.3557 x 10^{-3}
U_6	-3.6296 x 10^{-3}

The table indicates that the second eigenvector at $t = 0.776\ mm$ is the match to the second eigenvector at $t = 0.50\ mm$. New coefficients are calculated at $t = 0.776\ mm$ and a seventh-order curve fit is computed between $t = 0.50\ mm$ and

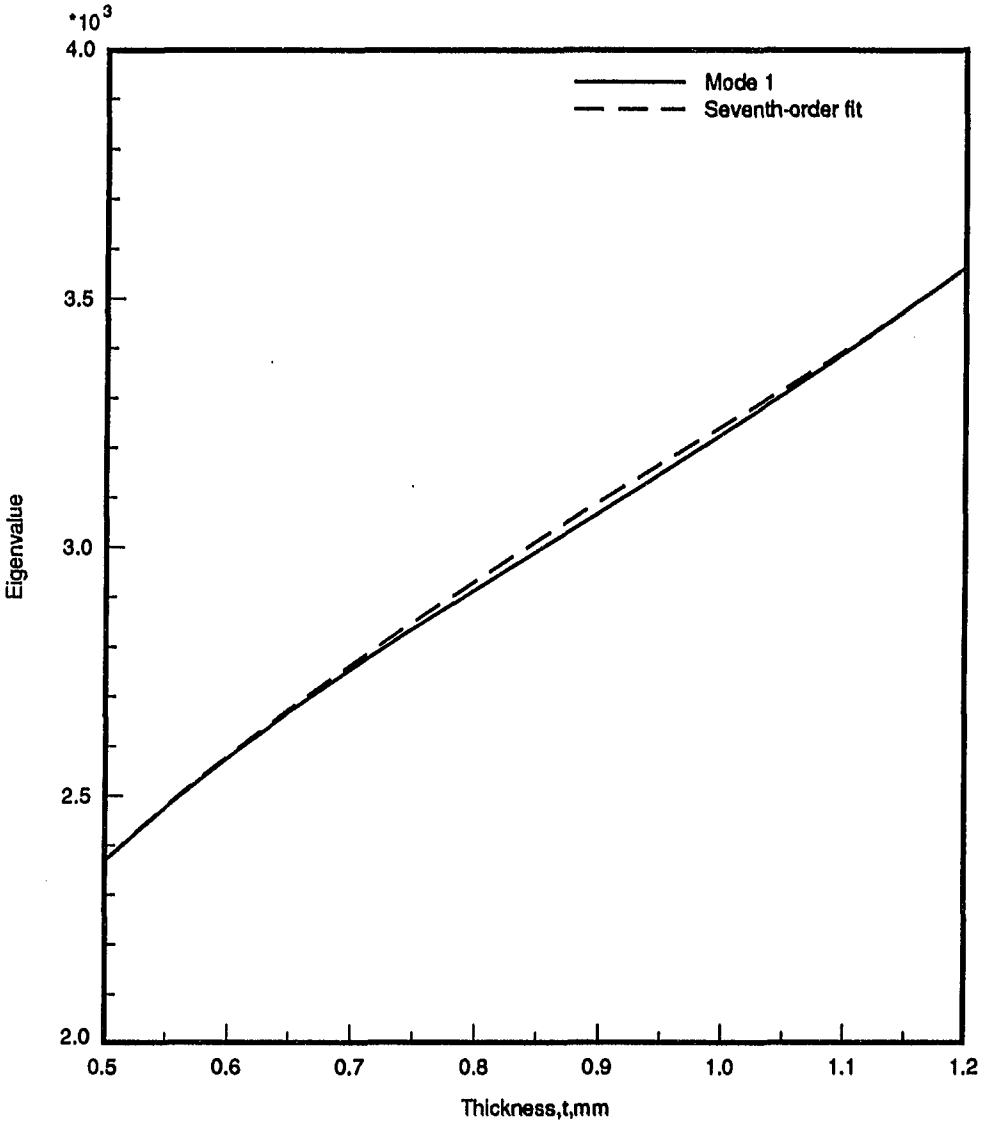

Figure 5.2: Mode 1 power series approximation: no re-solves

$t = 0.776\ mm$.

Using the new coefficients, a 3-term Taylor series and a 4-term Taylor series of the eigenvalue is formed at $t = 0.776\ mm$. The series differed by only 0.24% at $t = 1.20\ mm$ which is the end of the design range. M, Λ, and U are obtained at $t = 1.20\ mm$. The eigenvector was estimated with a 4-term Taylor series and the inner product of $(U_2^*)^T M U_p$ was formed at $t = 1.20\ mm$. The results are shown in Table 5.4.

Table 5.4: Mode 2 inner product of $(U_2^*)^T M U_p$ for $t_l = 1.20\ mm$

Inner product with	$(U_2^*)^T M U_p$
U_1	1.5885 x 10^{-2}
U_2	6.7989 x 10^{-13}
U_3	1.0054
U_4	-9.6746 x 10^{-14}
U_5	1.1345 x 10^{-2}
U_6	4.1583 x 10^{-2}

These values identify the mode 3 eigenvector at $t = 1.20\ mm$ as the match to the mode 2 eigenvector at $t = 0.776\ mm$. This indicates that within the range from $t = 0.776\ mm$ to $t = 1.20\ mm$ the eigenvalues have crossed. The mode 3 eigenvalue and eigenvector derivatives are computed at $t = 1.20\ mm$ and used with the mode 2 derivatives at $t = 0.776\ mm$ to form a seventh-order curve fit over this range.

Figure 5.3 presents the results of the piecewise fit for mode 2 over the entire design range. Note that the mode 2 eigenvalue becomes mode 3 eigenvalue for thickness values greater than $t = 1.00\ mm$.

Next, an 8-term/9-term series was used to see if adding more terms to the series would provide a good approximation across the design range without a re-solve. When the 8-term series was compared to the 9-term series, one re-solve was needed

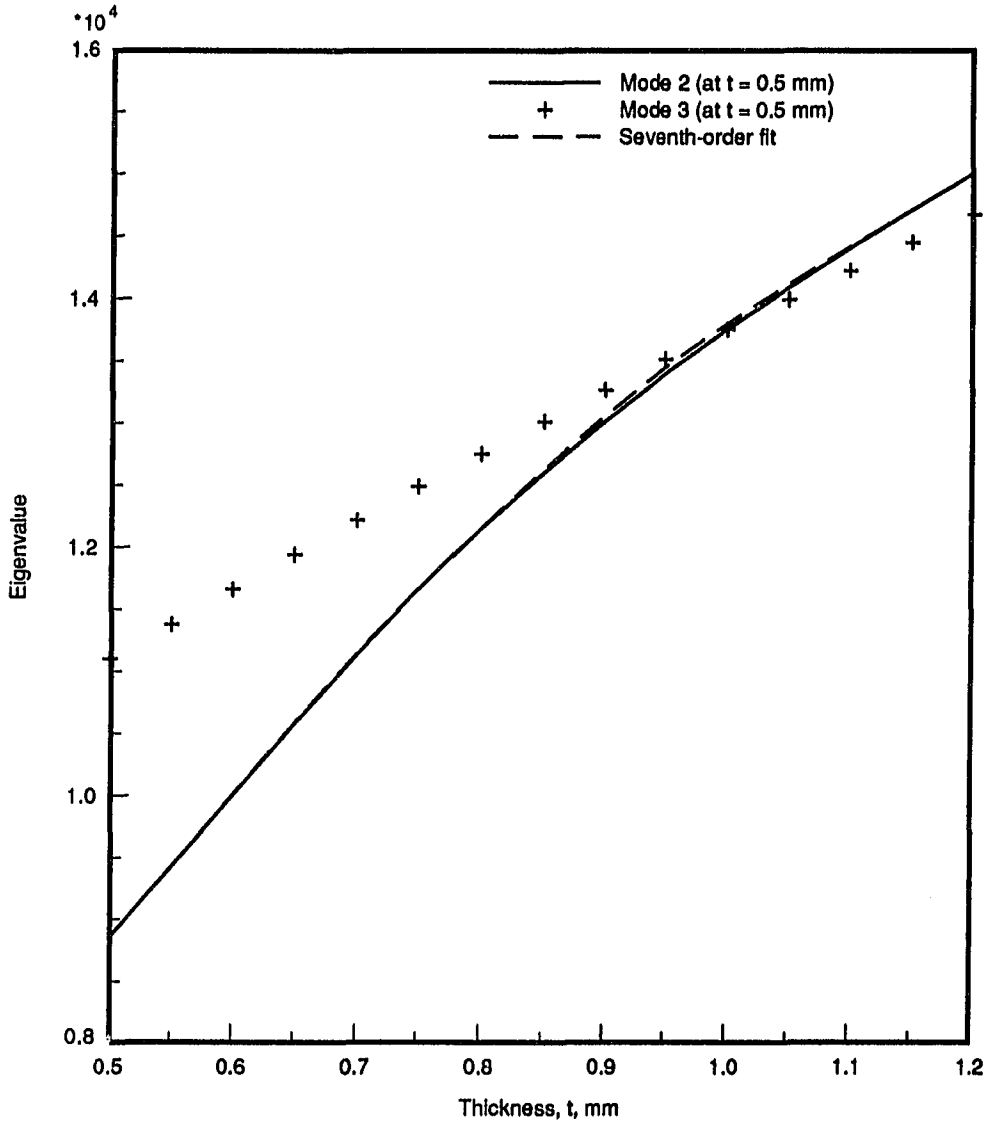

Figure 5.3: Mode 2 power series approximation: re-solve at $t = 0.776\ mm$

in the design range at $t = 0.985\ mm$. Therefore, there was no advantage to using a higher-order series in this case.

Curve fits for eigenvectors are calculated in a similar manner. Figures 5.4 and 5.5 present some results. The figures show the displacement of nodes lying along a cross-section of the plate at the center, extending from the variable thickness section to the constant thickness section. Figure 5.4 compares the mode 2 seventh-order fit based on the results of the 3-term/4-term series at $t = 0.65\ mm$ to the finite element solution at that thickness. Figure 5.5 presents a similar comparison for mode 2 at $t = 1.00\ mm$. These two thicknesses were chosen to illustrate the accuracy of the method because they are the thicknesses that lie in the middle of the re-solve ranges for mode 2 and therefore represent the worst case approximations. Because of the re-solve technique, the estimated eigenvectors will match the mode 2 eigenvectors at $t = 0.50\ mm$, $t = 0.776\ mm$, and $t = 1.20\ mm$.

This method has successfully arrived at adequate approximations over the entire design range for both mode 1 and mode 2. The cut off percents along with the inner product matching have successfully identified when to re-solve and which eigenvector and eigenvalue to use in the curve fit. For mode 1, the 3-term/4-term series was able to economically provide an adequate fit across the design range without a re-solve. For mode 2,both the 3-term/4-term series and the 8-term/9-term series required a re-solve within the design range.

Padé Approximants

The only difference in the procedure presented in the previous section for the power series approximation and the method used for the Padé approximants is that

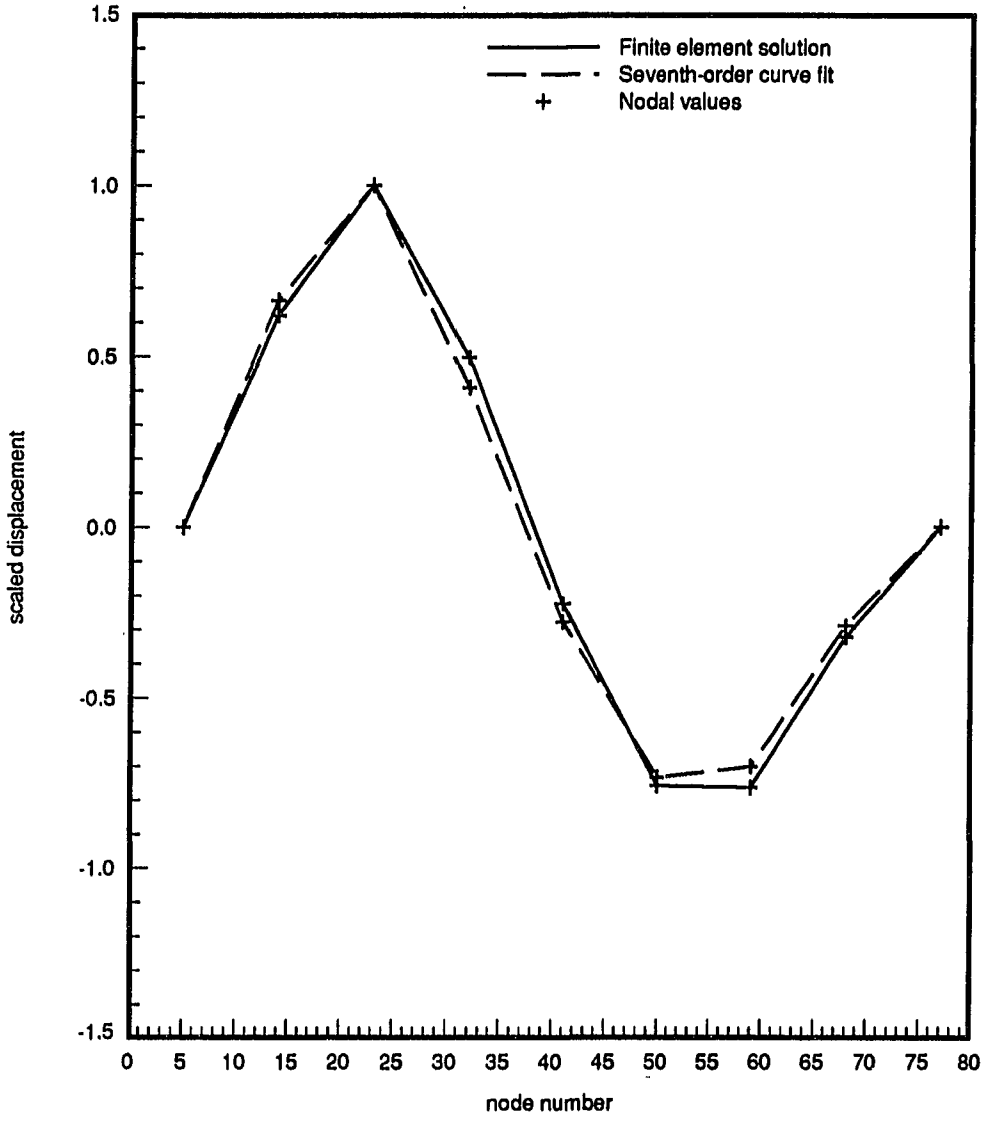

Figure 5.4: Mode 2 nodal displacement along a plate cross-section for $t = 0.65\ mm$

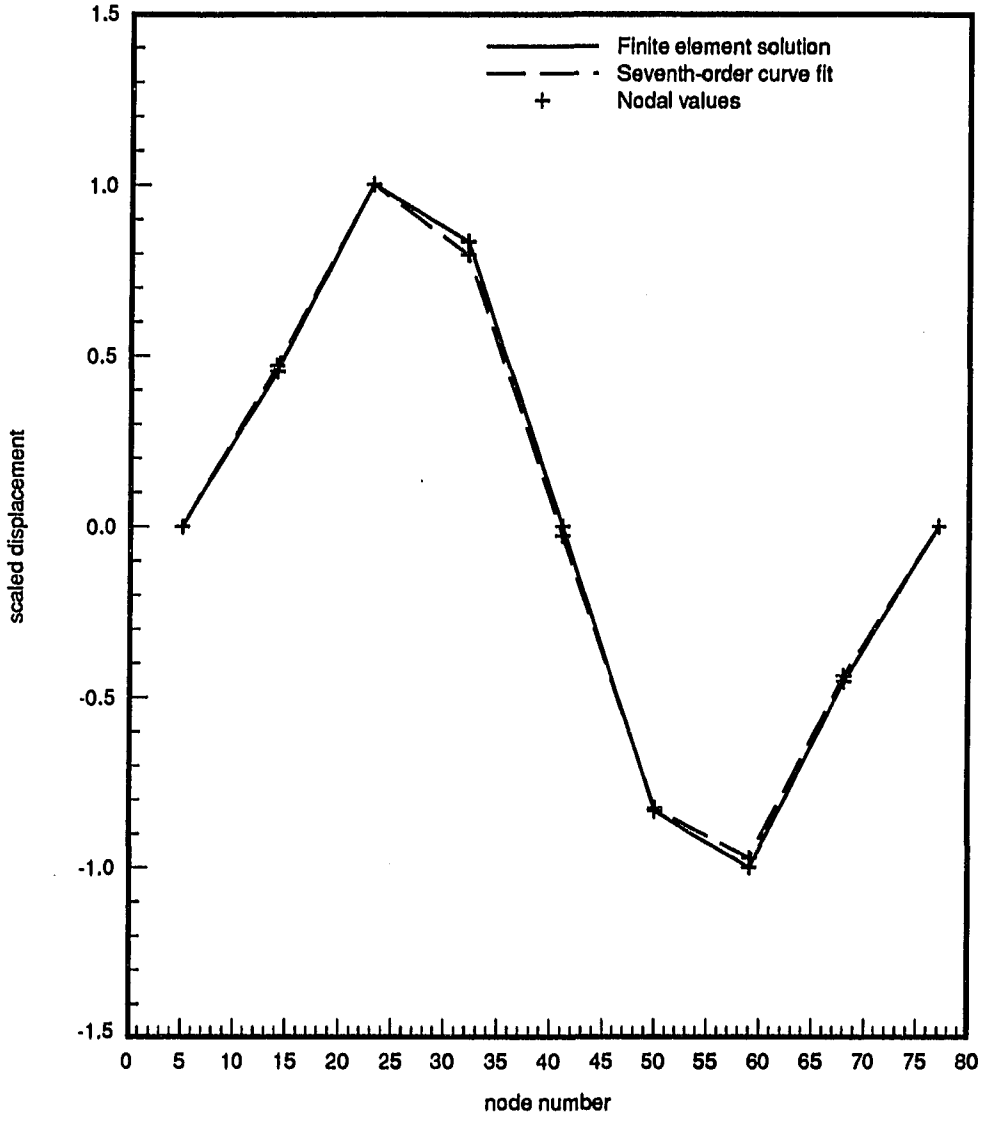

Figure 5.5: Mode 2 nodal displacement along a plate cross-section for $t = 1.0\ mm$

the the $R_{3,3}$ and the $R_{4,4}$ will be used for the comparison. First the $R_{3,3}$ and $R_{4,4}$ Padé approximants for the mode 1 eigenvalues from $t = 0.50\ mm$ to $t = 1.20\ mm$ were computed. This required calculating eight derivatives of the mode 1 eigenvalue at $t = 0.50\ mm$. The $R_{3,3}$ and the $R_{4,4}$ estimates differed by only 4.11% at the end of the range, indicating that a re-solve was not needed. The $R_{4,4}$ at $t = 1.20\ mm$ was computed for the eigenvector resulting in a value for U_1^*. The results of the inner product of $(U_1^*)^T M U_p$ is shown in Table 5.5.

Table 5.5: Mode 1 inner product of $(U_1^*)^T M U_p$ for $t_l = 1.20\ mm$ using Padé estimates

Inner product with	$(U_1^*)^T M U_p$
U_1	-0.9887
U_2	4.1909×10^{-9}
U_3	-3.9047×10^{-3}
U_4	-1.3038×10^{-8}
U_5	-5.0946×10^{-3}
U_6	2.4869×10^{-3}

The inner products indicate that the mode 1 eigenvector at $t = 1.20\ mm$ is the match to the mode 1 eigenvector at $t = 0.50\ mm$. The next step is to form a curve fit between the two points. A seventh-order curve fit was placed between $t = 0.50\ mm$ and $t = 1.20\ mm$. This results in the same fit as shown in Figure 5.2.

The Padé estimates for mode 2 are computed in a similar manner. Here again, at the end of the design range, $t = 1.20\ mm$, the $R_{3,3}$ and the $R_{4,4}$ differed by only 4.21%, therefore no re-solves are needed in the range. This is in contrast to the results presented for the 8-term/9-term series which required one re-solve in the range. The results of the inner product calculations for the $R_{3,3}$ and $R_{4,4}$ are shown in Table 5.6.

These calculations show that the mode 3 eigenvector at $t = 1.20\ mm$ is the match

Table 5.6: Mode 2 inner product of $(U_2^*)^T M U_p$ for $t_l = 1.20\ mm$ using Padé estimates

Inner product with	$(U_2^*)^T M U_p$
U_1	1.3634 x 10^{-2}
U_2	1.1175 x 10^{-8}
U_3	-0.9960
U_4	1.1175 x 10^{-8}
U_5	-2.7170 x 10^{-4}
U_6	-2.9950 x 10^{-3}

to the mode 2 eigenvector at $t = 0.50\ mm$. This result agrees with the findings of the inner product matching done using the Taylor series estimations. A seventh-order curve fit curve was computed between $t = 0.5\ mm$ and $t = 1.20\ mm$ and the results are shown in Figure 5.6.

These figures show Padé approximants have the ability to estimate eigenvalues over a very large design range.

Using Inner Product Matching for High Frequencies

The method of inner product matching was successful in identifying the correct matching frequency and mode shape for the curve fits for both modes 1 and 2. There may be some questions as to whether it will work as well for higher frequency modes. To address those questions, the inner product matching method was applied to the $9th$ mode of the plate. The 9^{th} mode was chosen because there exists a double root with the 10^{th} mode within the design range resulting in a reordered set of eigenvalues for designs where $t > 1.0\ mm$.

Using a 3-term/4-term power series for the projection, the 5% cut off percent occurred at $t = 0.648\ mm$. The results of the inner product matching at that

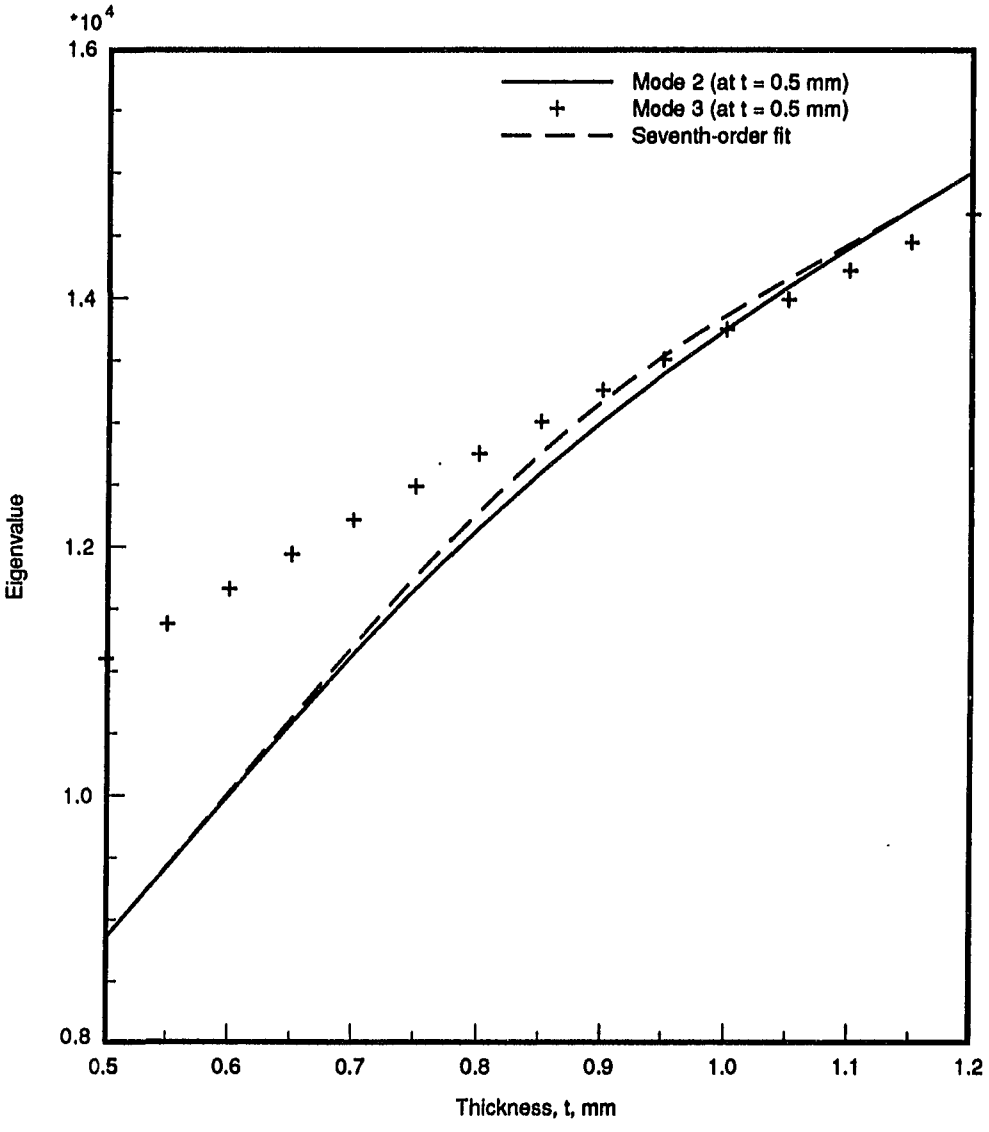

Figure 5.6: Mode 2 Padé approximants: no re-solves

point are presented in Table 5.7. The 9^{th} eigenvector was identified as the match at $t = 0.648\ mm$.

Table 5.7: Mode 9 inner product of $(U_9^*)^T M U_p$ for $t_l = 0.648\ mm$

Inner product with	$(U_9^*)^T M U_p$
U_1	8.129 x 10^{-4}
U_2	1.705 x 10^{-5}
U_3	4.708 x 10^{-15}
U_4	6.237 x 10^{-15}
U_5	6.471 x 10^{-3}
U_6	-2.035 x 10^{-3}
U_7	-5.810 x 10^{-14}
U_8	-0.104
U_9	1.050
U_{10}	1.387 x 10^{-13}

The new 3-term/4-term power series based at $t = 0.648\ mm$ indicated divergence at $t = 0.922\ mm$. The results of the inner product matching at that point are presented in Table 5.8. Once again the 9^{th} eigenvector was identified as the match.

Table 5.8: Mode 9 inner product of $(U_9^*)^T M U_p$ for $t_l = 0.922\ mm$

Inner product with	$(U_9^*)^T M U_p$
U_1	1.785 x 10^{-3}
U_2	-8.971 x 10^{-3}
U_3	2.5206 x 10^{-14}
U_4	-1.818 x 10^{-14}
U_5	-1.248 x 10^{-3}
U_6	2.768 x 10^{-3}
U_7	-3.054 x 10^{-2}
U_8	4.604 x 10^{-14}
U_9	-1.027
U_{10}	-2.019 x 10^{-13}

The next 3-term/4-term power series based at $t = 0.922\ mm$ was able to cover the remaining design space to $t = 1.20\ mm$ without the cut off percent exceeding 5%. The results of the inner product matching at $t = 1.20\ mm$ are presented in Table 5.9. Here the inner product matching method correctly identified the 10^{th} mode at $t = 1.20\ mm$ as the match to the 9^{th} mode at $t = 0.922\ mm$. These results are presented in Table 5.9.

Table 5.9: Mode 9 inner product of $(U_9^*)^T M U_p$ for $t_l = 1.20\ mm$

Inner product with	$(U_9^*)^T M U_p$
U_1	-2.605 x 10^{-4}
U_2	-5.391 x 10^{-14}
U_3	-1.621 x 10^{-3}
U_4	6.148 x 10^{-13}
U_5	-1.508 x 10^{-3}
U_6	-7.207 x 10^{-3}
U_7	-3.421 x 10^{-12}
U_8	-6.076 x 10^{-4}
U_9	-5.844 x 10^{-11}
U_{10}	-0.998

When examining a higher-order series for the 9^{th} mode, the 8-term/9-term series indicated divergence began to occur at $t = 0.675\ mm$. When the inner product was checked at that thickness, none of the eigenvectors were identified as the match. The range was cut in half and a re-solution was performed at $t = 0.5875\ mm$. A new inner product was formed at $t = 0.5875\ mm$ and the 9^{th} eigenvector was identified as the match. The next re-solve point occurred at $t = 0.8475\ mm$ and the 9^{th} eigenvector was again identified as the match. At $t = 1.04\ mm$ the inner product method correctly identified the 10^{th} eigenvector as the match to the 9^{th} eigenvector at $t = 0.8475\ mm$. The 8-term/9-term series was able to reach the end of the design

range with one more approximation from $t = 1.04\ mm$ to $t = 1.20\ mm$. This method required 4 re-solves to get a fit across the entire design range.

In contrast to the 8-term/9-term series, the $R_{3,3}/R_{4,4}$ Padé was able to span the entire design range from $t = 0.50\ mm$ to $t = 1.20\ mm$ without the need for a re-solve. At $t = 1.20\ mm$ the $R_{3,3}$ differed from the $R_{4,4}$ by 3.21%. At the end of the range, the inner product matching correctly identified the 10^{th} mode as the match to the 9^{th} mode at the beginning of the range. Figure 5.7 shows the correct finite element solutions for the 9^{th} and 10^{th} modes, the seventh-order curve fit between re-solve points obtained using the 3-term/4-term method, and the seventh-order curve fit between the endpoints of the design range.

This example shows that even for high modes, the inner product matching technique correctly identified the matching eigenvector and corresponding eigenvalue. In addition, the Padé method proved to be a powerful tool for the high modes.

Comparison of Power Series Methods to Padé Approximant Methods

For the plate model, the two methods can be compared based on the computation time required to obtain a good approximation of eigenvalues and eigenvectors across the design range. For mode 1, both methods were able to span the entire range of design values without a re-solve. In this case, the difference in computation time is due to the cost of calculating the derivatives needed for the approximation. To calculate the $R_{4,4}$ or the 9-term series, eight derivatives are needed. The 4-term power series requires only three derivatives. The Padé and the 9-term series therefore require calculation of five more derivatives than the 4-term power series method.

On a DECstation 3100 workstation using MSC/Nastran DMAP software for the

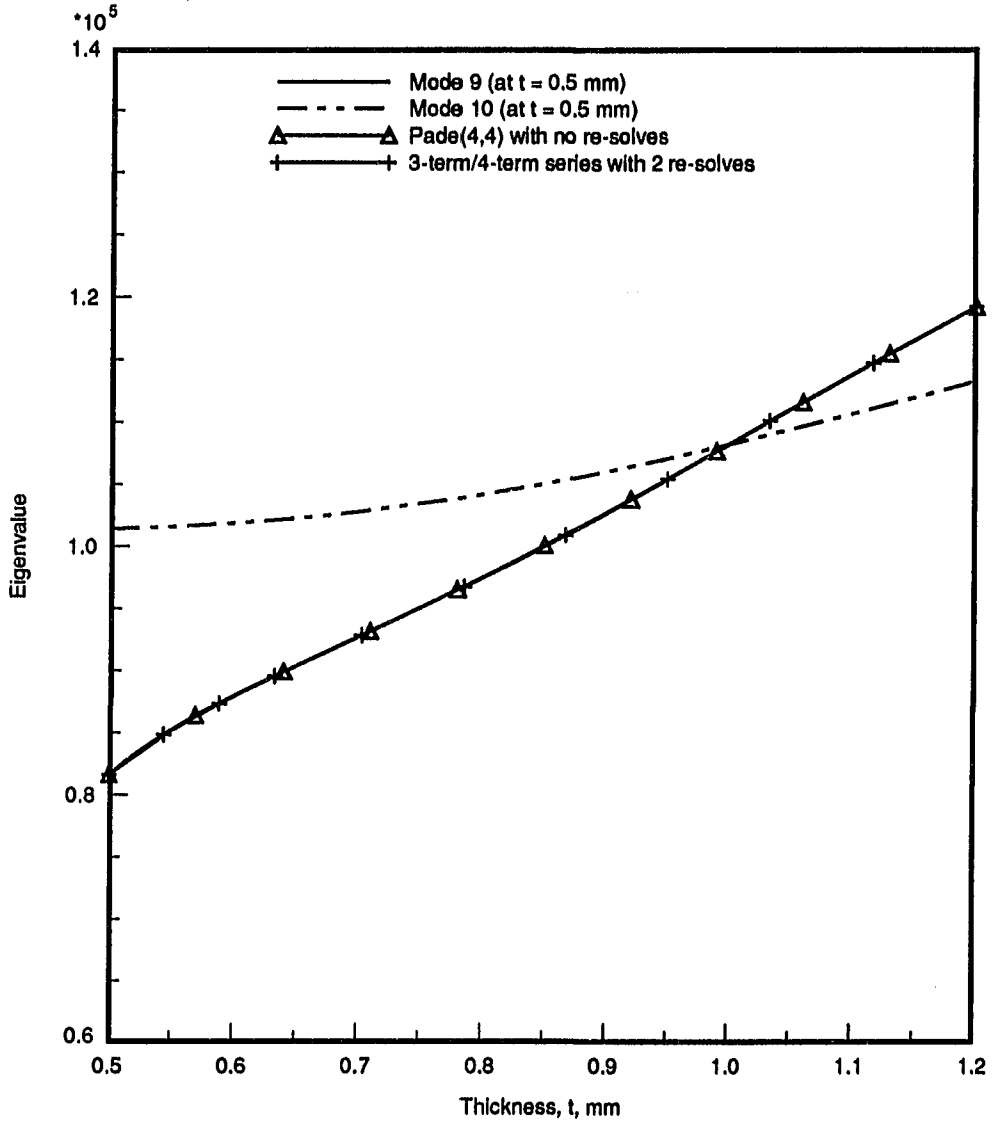

Figure 5.7: Mode 9 Padé and power series approximations

calculations, the CPU time required to obtain a set of eigenvalue and eigenvector derivatives remained relatively constant at 2.3 seconds per set. Therefore, in approximating the eigenvalues across the design range, the Padé approximant method required about 11.5 seconds more than the power series method for mode 1. The 3-term/4-term series was the most economical method in this case.

For mode 2, the Padé method was able to provide a good fit over the entire range without a re-solve. The 3-term/4-term power series method required one more re-solve, calculation of new mass and stiffness derivatives at the re-solve point, and calculation of new series coefficients. This amounted to an additional 71.3 seconds.

Since the $R_{4,4}$ Padé requires eight derivatives, a comparison for mode 2 was also made using an 8-term/9-term Taylor series because the 9-term series also requires eight derivatives of the eigenvalue. The 8-term/9-term series was not able to span the entire design range for mode 2 and a re-solve was indicated at $t = 0.00111\ mm$. Therefore, the 8-term/9-term series was even more costly than the 3-term/4-term series due to the additional derivatives required.

Table 5.10 presents a breakdown of the time required for the mode 2 approximation using both the power series method and the Padé method. Because of the re-solve needed for the mode 2 power series, that method required more time than the Padé method.

For mode 9, the 3-term/4-term method required four solutions and twelve derivative calculations. The 8-term/9-term method required six solutions and thirty-five derivative calculations, while the Padé method only required two solutions and eleven derivative calculations. The Padé method is the clear choice for this higher mode.

The next chapter presents conclusions and a discussion of future areas of work.

Table 5.10: Computation time required for Padé method and power series methods for mode 2

Operation	Padé method	4-term series	9-term series
Initial solution	32.4 s	32.4 s	32.4 s
M and K derivatives	22.0 s	22.0 s	22.0 s
Derivative pre-process	21.5 s	21.5 s	21.5 s
Derivative calculations @ 2.3 s each	18.4 s	6.9 s	18.4 s
Re-solve	-	32.4 s	32.4 s
M and K derivatives	-	22.0 s	22.0 s
Derivative pre-process	-	21.5 s	21.5 s
Derivative calculations	-	6.9 s	6.9 s
End solution	32.4 s	32.4 s	32.4 s
End derivative pre-process	21.5 s	21.5 s	21.5 s
End derivative calculations	6.9 s	6.9 s	6.9 s
Total	155.1 s	226.4 s	237.9 s

CHAPTER 6. CONCLUSIONS AND FUTURE WORK

While the methods developed here deal with one design parameter, other multi-parameter methods can be used in conjunction with this method for multi-parameter optimization. Several authors have proposed first formulating the objective function using linear sensitivities with respect to multiple design variables. After an acceptable direction of search has been identified, the problem is reformulated using nonlinear sensitivities in one design variable. The methods laid out in this thesis provide an improved method to carry out the nonlinear portion of the optimization.

These two examples have illustrated that power series approximation methods or Padé approximant methods combined with curve fit techniques provide accurate eigenvalue and eigenvector approximations across large design changes of a single design parameter. The methods of inner product matching and the use of cut off percents proved to be effective methods to aid in eigenvector matching and determining when to perform a re-solve within the design region.

The Padé approximant method has been shown to be economical for large design changes where the power series cannot span the entire design range. This is especially true for cases where the cost of the re-solve is relatively high compared to the cost of calculating derivatives.

The inner product matching technique proved to be a powerful tool when used

to identify matching eigenvectors and eigenvalues for a curve fit. In addition, the technique provided a check on the accuracy of the power series or Padé approximation of the eigenvector at the re-solve point.

One difficulty that may be encountered when using Padé methods is that convergence is not guaranteed for eigenvalue problems. The possibility exists that for a different problem the Padé may not be able to span the range without a re-solve.

Improvements on this method bear further investigation. More experience applying this method to large systems that possess wide variations in either the eigenvalues or eigenvectors will provide additional insight into the advantages of the power series method over the Padé method or vice versa. Additional work is also needed concerning the determination of the mass and stiffness matrices derivatives. The present method requires that the derivatives of every element to be re-calculated at each re-solve point. It will be useful to obtain these derivatives by recomputing only the elements of each matrix which are affected by the design change, thereby reducing the computation time required for each re-solve.

Further work is needed to combine these methods with computer graphics to produce a program for design optimization. The intent is to develop the graphics that allow a designer to view the initial mode shape and subsequent mode shapes interactively during the course of the optimization. The focus of this research will be to facilitate visual feedback to support interactive design optimization of structural systems.

BIBLIOGRAPHY

[1] Adelman, Howard M. and Raphael T. Haftka. "Sensitivity Analysis of Discrete Structural Systems." *AIAA Journal*, 24, No. 5, 1986, 823-832.

[2] Wittrick, W.H. "Rates of Change of Eigenvalues, With Reference to Buckling and Vibration Problems." *Journal of the Royal Aeronautical Society*, 66, 1962, 590-591.

[3] Jacobi, C.G.J. "Uber ein leichtes Verfahren die in der Theorie der Saecularstoerungen vorkommenden Gleichungen numerisch aufzuloesen." *Zeitschrift für Reine und Angewandte Mathematik*, 30, 1846, 51-95. also NASA TT-F-13666, N71-28134, June 1971, 1-50.

[4] Lancaster, P. "On Eigenvalues of Matrices Dependent on a Parameter." *Numerische Mathematik*, 6, 1984, 377-387.

[5] Fox, R.L. and M.P. Kapoor. "Rates of Change of Eigenvalues and Eigenvectors." *AIAA Journal*, 6, No. 12, 1968, 2426-2429.

[6] Rogers, L.C. "Derivatives of Eigenvalues and Eigenvectors." *AIAA Journal*, 8, No. 5, 1970, 943-944.

[7] Plaut, R.H., and K. Huseyin. "Derivatives of Eigenvalues and Eigenvectors in Non-Self-Adjoint Systems." *AIAA Journal*, 11, No. 2, 1973, 250-251.

[8] Rudisill, Carl S. and Kumar G. Bhatia. "Second Derivatives of the Flutter Velocity and the Optimization of Aircraft Structures." *AIAA Journal*, 10, No. 12, 1972, 1569-1572.

[9] Murthy, Durbha V. and Raphael T. Haftka. "Survey of Methods for Calculating Sensitivity of General Eigenproblems." Sensitivity Analysis in Engineering (symposium), NASA Langley Research Center, Hampton, VA, Feb. 1987. NASA CP-2457, NTIS N87-18867.

[10] Storaasli, Olaf O. and Jaroslaw Sobieszczanski. "On the Accuracy of the Taylor Approximation for Structure Resizing." *AIAA Journal*, 12, No. 2, 1974, 231-233.

[11] Kirsch, U. "Approximate Structural Reanalysis Based on Series Expansion." *Computer Methods in Applied Mechanics and Engineering*, 26, 1981, 205-223.

[12] Haug, Edward J. "Second-Order Design Sensitivity Analysis of Structural Systems." *AIAA Journal*, 19, No. 8, 1981, 1087-1088.

[13] Haftka, Raphael T. "Second-Order Sensitivity Derivatives in Structural Analysis." *AIAA Journal*, 20, No. 12, 1982, 1765-1766.

[14] Vanderplaats, Garret N. and Noriaki Yoshida. "Efficient Calculation of Optimum Design Sensitivity." *AIAA Journal*, 23, No. 11, 1985, 1798-1803.

[15] Sobieszczanski-Sobieski, Jaroslaw. "Higher Order Sensitivity Analysis of Complex, Coupled Systems." *AIAA Journal*, 28, No. 4, 1990, 756-758.

[16] Rizai, Matt N. and James E. Bernard. "An Efficient Method to Predict the Effect of Design Modifications." *Journal of Mechanisms, Transmissions, and Automation in Design*, 109, 1987, 377-384.

[17] Somayajula, Gopichand and Jim Bernard. "Design Optimization of Structures Subject to Static and Dynamic Constraints." *Finite Elements in Analysis and Design*, 5, 1989, 281-289.

[18] Garg, Subhash. "Derivatives of Eigensolutions for a General Matrix." *AIAA Journal*, 11, No. 8, 1973, 1191-1194.

[19] Rudisill Carl S. "Derivatives of Eigenvalues and Eigenvectors for a General Matrix." *AIAA Journal*, 12, No. 5, 1974, 721-722.

[20] Nelson, R.B. "Simplified Calculation of Eigenvector Derivatives." *AIAA Journal*, 14, No. 9, 1976, 1201-1205.

[21] Cardani, C. and P. Mantegazza. "Calculation of Eigenvalue and Eigenvector Derivatives for Algebraic Flutter and Divergence Eigenproblems." *AIAA Journal*, 17, 1979, 408-412.

[22] Haug, Edward J. and Jasbir S. Arora. "Design Sensitivity Analysis of Elastic Mechanical Systems." *Computer Methods in Applied Mechanics and Engineering*, 15, 1978, 35-62.

[23] Ojalvo, I.U. "Efficient Computation of Mode-Shape Derivatives for Large Dynamic Systems." *AIAA Journal*, 25, No. 10, 1987, 1386-1390.

[24] Whitesell, J.E. "Design Sensitivity in Dynamical Systems." Ph.D. thesis, Mechanical Engineering Department, Michigan State University, Ann Arbor, MI, 1980.

[25] Bernard, J.E., S.K. Kwon, and J.A. Wilson. "Differentiation of Mass Stiffness Matrices for High Order Sensitivity Calculations in Finite Element Based Equilibrium Problems." *Proceedings, ASME Design Automation Conference*, ASME, 1990, to be published, *Journal of Mechanical Design.*

[26] Whitesell, J.E. "Rational Approximants in Structural Design Reanalysis." *Journal of Mechanisms, Transmissions, and Automation in Design*, 106, 1984, 114-118.

[27] Kwon, S.K. and J.E. Bernard. "Design Optimization Based on Padé Expansions." *Proceedings 1991 MSC World User's Conference*, March 11-15, 1991, to be published in *Finite Elements in Analysis and Design.*

[28] Vance, J.M. and J.E. Bernard "Interactive Analysis of Vibration Modes Using Approximation Algorithms and Computer Graphics." *Computer-Aided Design*, 21, No. 7, 1989, 430-434.

[29] Starkey, J.M. and J.E. Bernard. "A Constraint Function Technique for Improved Structural Dynamics." *Journal of Vibrations, Acoustics, Stress, and Reliability in Design*, ASME, 108, 1986, 101-106.

[30] *MSC/NASTRAN User's Manual, Version 66A*, The MacNeal-Schwendler Corporation, Los Angeles, CA, November 1989.

[31] Brezinski, Claude. "History of Continued Fractions and Padé Approximants." *Springer Series in Computational Mathematics 12*, Springer Verlag, New York, 1991.

[32] *I-DEAS Finite Element Modeling User's Guide, Version 5*, Structural Dynamics Research Corporation, Milford, Ohio, 1990.